

Sample preparation strategies for efficient correlation of 3D SIM and soft X-ray tomography data at cryogenic temperatures.

Chidinma A. Okolo^{1*}, Ilias Kounatidis^{1*}, Johannes Groen^{2*}, Kamal L. Nahas^{1,3}, Stefan Balint⁴, Thomas M. Fish¹, Mohamed A. Koronfel¹, Aitziber L. Cortajarena^{5,6}, Ian M. Dobbie⁷, Eva Pereiro² and Maria Harkiolaki^{1§}.

¹ Beamline B24, Diamond Light Source, Harwell Science and Innovation Campus, Didcot, Oxfordshire, OX11 0DE, United Kingdom.

² Beamline 09 - MISTRAL, ALBA Synchrotron, Carrer de la Llum 2-26, Cerdanyola del Vallès, 08290 Barcelona, Spain.

³ Division of Virology, Department of Pathology, University of Cambridge, Tennis Court Road, Cambridge, CB2 1QP, United Kingdom.

⁴ Kennedy Institute of Rheumatology, University of Oxford, Roosevelt Drive Headington, Oxford, OX3 7FY, United Kingdom.

⁵ Center for Cooperative Research in Biomaterials (CIC biomaGUNE), Basque Research and Technology Alliance (BRTA), Paseo de Miramón 182, 20014, Donostia San Sebastián, Spain.

⁶ Ikerbasque, Basque Foundation for Science, M^a Díaz de Haro 3, 48013 Bilbao, Spain.

⁷ Micron Advanced Imaging Consortium, Department of Biochemistry, University of Oxford, South Parks Rd, Oxford OX1 3QU, United Kingdom.

** Joint first authors*

§ Corresponding author, email: maria.harkiolaki@diamond.ac.uk

KEYWORDS Visible light fluorescence microscopy, soft X-ray tomography, SXT, correlative light and X-ray tomography, CLXT, structured illumination, SIM, fiducials, fluorescent nanoparticles, cryo-imaging

EDITORIAL SUMMARY This protocol describes sample preparation strategies for correlative 3D cryo-SIM and cryo soft X-ray tomography. In addition, the authors provide a direct comparison and recommendations regarding the selection and use of fiducials for 3D correlation.

TWEET A new protocol for sample preparation and fiducial selection for correlative cryo-SIM and cryo-soft X-ray tomography. #CLXT #cryoimaging #cellstructure #correlativeimaging

COVER TEASER Correlative cryo-SIM and cryo-soft X-ray tomography

Abstract

3D correlative microscopy methods have revolutionised biomedical research allowing the acquisition of multi-dimensional information to gain an in-depth understanding of biological systems. With the advent of relevant cryo-preservation methods, correlative imaging of cryogenically preserved samples has led to nanometre resolution imaging (2-50 nm) under harsh imaging regimes such as electron and soft X-ray tomography. These methods have now been combined with conventional and super resolution fluorescence imaging at cryogenic temperatures to augment information content from a given sample resulting in the immediate requirement for protocols that facilitate hassle-free unambiguous cross correlation between microscopes. We present here sample preparation strategies and a direct comparison of different working fiducialisation regimes that facilitate 3D correlation of cryo-structured illumination microscopy and cryo-soft X-ray tomography. Our protocol has been tested at two synchrotron beamlines (B24 at Diamond Light Source in the UK and BL09 Mistral at ALBA in Spain) and has led to the development of a decision aid that facilitates experimental design with the strategic use of markers based on project requirements. This protocol takes between 1.5 hours and 3.5 days to complete, depending on the cell populations used (adherent cells may require several days to grow on sample carriers).

Introduction

Correlative imaging involves the spatial integration of imaging data collected by different microscopy techniques from a single specimen. Its power relies on its ability to bring together data from a variety of cell features captured using different contrasting methods. This way, high lateral, axial and spatiotemporal resolutions can be achieved when imaging the same cellular areas and capturing structures or processes across different scales at different time points and over a range of wavelengths, while also delivering volumetric information¹⁻⁴. Since correlative imaging was first reported in 1965⁵, when the term correlative light and electron microscopy (CLEM) was coined, techniques have evolved and matured but have also led to challenges in the quest to capture and cross-reference native cell structures using different microscopy platforms⁶⁻⁹. A significant advance in the field was marked by the advent of cryo-imaging which enabled nanometre resolution with ionizing illuminating radiation at near-physiological conditions¹⁰⁻¹³. Nowadays, cryogenic temperatures are routinely used to capture information in electron microscopy¹³⁻¹⁸, X-ray microscopy and in particular soft X-ray tomography¹⁹⁻²⁵ and, visible light fluorescence microscopy^{16,26-29}. In the past, to suit the requirements of different imaging techniques, samples often needed to be processed heavily between data collection on different microscopes leading to data correlation that was susceptible to interference and artefacts. Presently, developments focus on direct and accurate correlation by imaging the same field of view within a sample with more than one microscopy technique, without incurring changes to cell ultrastructure through chemical embedding, fixation, dehydration or other modifications. This has been demonstrated in our recent work, where we developed a novel correlative imaging scheme to image whole vitrified cells using both cryo-structured illumination microscopy (cryoSIM) in 3D and cryo-soft X-ray tomography (cryoSXT)²². In this approach, we adapted both 3D imaging techniques to allow correlative 3D cryo-imaging without process-induced sample degradation. Combinations of soft X-ray and visible light fluorescence microscopy are collectively called Correlative Light and X-ray Tomography (CLXT)^{30,31}.

Given the constant demand for easily accessible and user-friendly methodologies, a clear and consistent strategy to ease the processing and correlation for CLXT imaging data is required. A major step forward in this direction is the development of clear and unambiguous protocols that ease data reconstruction and data correlation across microscopies by paying attention to a number of considerations. First, sample preparation and sample support (holders and support surfaces) used should be suitable for all the imaging modalities within the scheme^{32,33}. In addition, the workflow should be designed in such a way that a preceding imaging technique does not deteriorate sample quality or compromise incorporated reagents needed

for the success of the next method. It is also essential to maintain cryogenic temperatures across methods to ensure the integrity and structure of the biological sample. A major challenge in CLXT is that each microscopy method relies on different properties, reagents, or inherent sample characteristics to deliver sufficient contrast in the images captured. For example, soft X-ray absorption-contrast imaging records the preferential absorption of X-rays by carbon-rich biological structures^{19,20} while fluorescence imaging records the location of light emitting centres within a cell, irrespective of carbon content in the area^{34,35}. These data may well originate from the exact same area within a cell; however, they are likely to bear no similarity in the recorded images, leaving the researcher without reference points to allow the useful association of the information captured. This brings about the absolute need for positional markers (fiducials) visible across the correlative scheme that can serve as universal points of reference for 3D imaging data alignment^{1,13,36–39}.

In this protocol, we describe how to prepare sample supports and samples (adherent cells or cells in suspension) for correlative imaging using our 3D CLXT platform (cryoSIM and cryoSXT). Furthermore, to enable informed sample preparation, we evaluate different fiducialisation approaches for data processing and correlation of 3D imaging volumes between cryoSIM and cryoSXT.

Development of the protocol

The design, installation and development of the imaging modalities (3D cryoSIM and cryoSXT) which are employed in our correlative imaging workflow have been previously described^{21,22,26,40,41}. The established workflow at synchrotron facilities that provide access to these microscopes starts with sample preparation on EM grids followed by addition or expression of fluorophores, addition of image registration markers and cryo-fixation, mapping of samples using conventional widefield microscopy, 3D cryoSIM data collection, cryoSXT data collection and CLXT data processing and registration. SIM is a super resolution fluorescence imaging method that employs light with a known structure to illuminate and excite fluorophores within a sample. This results in emitted light that contains interference patterns which can be used to extrapolate structural information beyond the diffraction limit (resolution of 200 nm laterally and 520 nm axially given a NA of 0.9 at 525 nm)²². SIM can be used as a 3D imaging tool by using three beam orders (-1/0/+1) and by moving the sample along the beam path thus bringing consecutive slices of the target object in focus⁴². The implementation of this method for the study of samples under cryogenic conditions has been documented recently²⁶ and promises to become an absolutely essential partner for 3D correlative cryo-imaging. CryoSXT, on the other hand, has been in development for over a decade^{9,30–35}. It is, primarily, a synchrotron-

based technique that relies on the absorption of soft X-rays in the water window energy range (284 eV to 543 eV) as they transverse biological material whereupon, carbon-rich biological structures absorb X-rays heavily compared to their oxygen-rich environment leaving their likeness on the transmission signal recorded on an X-ray detector. Depending on the optics used, cryoSXT can deliver lateral resolution of up to 25 nm half pitch^{20,43,44}, thereby bridging the extant resolution gap between visible light diffraction-limited fluorescence light microscopy and electron microscopy. In cryoSXT, resolution is limited by the available X-ray optics as well as by the data collection schemes (full or partial tilt series) and signal-to-noise values achievable in fully hydrated relatively thick biological samples (up to 10 μm). The correlation of cryoSIM and cryoSXT results in augmented and enriched information that is spatially localised in the 3D cellular volume, allowing identification and quantitation of cellular features beyond what is achievable with either of these techniques alone. ... Note that 3D correlation of data from two microscopes that capture fundamentally different information (visible light emitted from fluorophores versus carbon density distribution in this case), even when such information originates from the exact same area within a cell, is a challenging task given that features highlighted in one dataset are not visible in the other. To achieve reliable volume correlation, positional markers that are visible in both modalities need to be included and a comprehensive approach to incorporating these in samples is required. The protocols presented here (**Figure 1**) address this requirement by optimising the decision process and the steps required in sample preparation for CLXT.

In our approach, 3D cryoSIM and cryoSXT data are acquired at different times using different microscopes and acquisition software, which means that samples are loaded on microscopes multiple times and at different orientations resulting in the requirement to derive accurate transformation matrices that relates the position of cellular features in one data set with respect to the other. To achieve this, it is essential to incorporate fiducials within the sample or in proximal areas of the sample support which act as distinctive landmarks that guide data correlation⁴⁵. An ideal fiducial should be visible and stable in both imaging modalities³¹, by having both a high fluorescence quantum yield (to be visible in cryoSIM data) and good X-ray absorption contrast (to be visible in cryoSXT data). At this juncture, it is important to note that fiducials are not only necessary for correlation, but also required for accurate alignment of X-ray projections to a common rotation axis for cryoSXT^{21,41}. To date, non-fluorescent gold (Au) nanoparticles, 100-250 nm in diameter, have been traditionally used as alignment fiducials. These are well suited for alignment prior to reconstruction of X-ray tilt series projections to 3D tomograms as they are highly absorbent with well-defined geometry, but are not ideal for 2D or 3D correlation cryoSIM data to X-ray data because they generally lack fluorescence

(although plasmon resonance has been observed sporadically) and can display batch specific adverse behaviour such as clumping^{46–49}.

In the Experimental Design section of this protocol, we provide a direct comparison of a selection of available sample fiducialisation approaches for CLXT (**Figure 2**) and present data that exemplifies their application and potential. Moreover, we offer a decision matrix (**Figure 3**) that allows users to make informed decisions about their sample preparation according to the imaging method they will be using and their particular sample and project requirements.

Overview of the Procedure

Our experimental workflow (**Figure 1**) starts with the growth or deposition of samples (primary or immortalised biological samples such as mammalian and insect cells, bacteria, archaea, algae, viral particles, parasites, exosomes or similar) on pre-coated (Step 1) flat gold EM grids with a thin perforated carbon film as a support surface (Step 2). Before cryo-fixation, live-cell microscopy such as conventional brightfield, fluorescence imaging or confocal imaging is advisable to provide snapshots of the subject matter before vitrification and transitioning to cryogenic temperatures. These snapshots will allow checking for cell confluency or relevant time conditions in a process. To enable future correlation of images, appropriate fiducialisation of samples is a crucial step which involves the addition of cell-independent markers that distribute evenly across the sample in all three dimensions as well as the labelling of distinct organelles within the target population (Steps 3-10) to allow both rough and fine alignment *in silico*. Following vitrification (Steps 11-31), samples are inspected for ice thickness, carbon film preservation, as well as cell and fluorophore distribution (Steps 32-46), and mapped (to enable future registration of images and aid positioning on relevant regions of interest) using conventional cryo-imaging equipment such as an epifluorescence optical microscope equipped with a cryo-stage (Steps. 47-53). The vitrified and mapped samples can then be taken for 3D cryoSIM and cryoSXT as described elsewhere²².

Applications of the method

The method presented here can be applied to sample preparation for a number of applications and is also compatible with other imaging techniques. For example, in addition to cultured cells, cryoSXT can also be used to image several microns of tissue cryopreserved by high-pressure freezing⁵⁰ and some of the fiducialisation aspects of this work could apply to such samples too (involving deposition of fiducials rather than intracellular delivery). Furthermore,

spectroscopic imaging (2D or 3D) over a range of X-ray wavelengths at elemental absorption edges could be incorporated in the imaging modalities that can be serviced by our fiducialisation regime (provided radiation damage can be mitigated). With tuneable-energy X-ray absorption spectroscopy and differential absorption tomography, the localization, composition and information of chemical elements within biological samples can be mined and analysed^{19,40,51}. In turn, the 3D cryoSIM imaging platform, is part of a dual imaging platform, comprising cryoSIM and cryoSTORM (direct stochastic optical reconstruction microscopy) capabilities. dSTORM will also require that samples are well fiducialised for correlative purposes as indeed any other 3D cryo-imaging method that can adopt EM grids as sample carriers²².

Within correlative 3D cryo-imaging sample preparation schemes, the fiducialisation approach described in this protocol would be well suited to correlative approaches that use different contrasting regimes (for example, cryo-FIB SEM prior to cryo-ET). In general, the fiducialisation process presented here can be conceivably adopted where needed as cross registration tools for multimodal imaging of cells and cell populations at cryogenic temperatures.

Comparison with other methods

There are many biological correlative imaging approaches in cryogenic conditions available nowadays, and each of them is tackling different ranges of sample thickness, resolutions and also information. The relatively novel combination of cryoSXT and cryo hard X-ray fluorescence tomography⁵² for example allows high chemical sensitivity inside the 3D cellular structure. Our approach (cryoSIM with cryoSXT) allows imaging of cellular structures at medium resolution (25-50 nm) in up to 10 μ m thick samples with localisation of specific organelles, macromolecules or events via their fluorescence signal to a resolution of better than 200nm. The choice of developing 3D cryoSIM, among other super resolution techniques available, in this scheme is explained primarily by the need for a high throughput technique that allows the imaging of several sample conditions in a short period of time (few days at a synchrotron facility). Note as well that, commercial instruments working at cryogenic temperatures are scarce and still under development. Future advances and new developments in super resolution techniques will certainly come in the following years, which will hopefully further improve the resolution gap in CLXT.

A number of approaches in biological imaging are currently being used to bring about biological image registration in 2D and 3D. Most commonly, samples of a target cell population are prepared in parallel and then taken to different microscopes to inspect⁵³. Data collected by

different microscopy methods on similar samples are then inspected and features that can be detected in both are used to infer correlation. CLXT provides the extra advantage that the same cellular area can be imaged sequentially and therefore extraneous features that indirectly inform correlation are not needed. The same cell and the same regions within and across cells are imaged and therefore registration only requires a single translation-rotation-scale transformation matrix per data and a set of distinct features within the sample suffice to correlate 3D volumes (the latter being the focus of this protocol).

A relevant current field which could benefit from the CLXT protocol detailed here is cryo electron tomography (cryoET). For example, in workflows where scanning electron microscopy and focused ion milling precedes cryoET, fluorescently tagged macromolecules contained within cells can direct the production of lamellas in areas of relevant biological interest. Subsequent cryo-ET on those lamellas would benefit from correlation to the original fluorescent signal⁵⁴. In such an occasion, protocols such as ours could be adapted to enable data correlation in an efficient way. CLXT and CLEM methods at times share the same sample support (EM grids) and sample preparation steps (blotting and cryopreservation) and, commercial fiducials used in this protocol such as gold nanoparticles are also common reagents (although sizes required vary greatly). Other reagents used in our protocol, such as fluorescently tagged plastic or metal nanoparticles with embedded or attached fluorophores, are also used in CLEM to deliver registration markers that bridge resolution and contrast barriers⁵⁵. It is noteworthy that stage or sample holder-specific markers have been used previously to provide a coarse image registration before finer nanoparticle fiducials embedded within the sample are used for data registration⁵⁶. This is not currently implemented in synchrotron-based CLXT but could prove a valuable addition in the future.

Within the field of CLXT, fiducialisation approaches so far have included the manual overlay of gross morphological sample carrier and cell features^{30,57} alongside the employ of fluorescent nanoparticles⁵⁸ and appropriately labelled cellular features^{22,59-61}. What has been missing in the field is a concise strategy towards the deployment of the current arsenal of fiducials commercially available. Moreover, the cryo-fluorescence imaging methods in CLXT to date only provided 2D imaging and hence had fewer requirements lacking depth localization information.

Limitations of the protocol

Complete vitrification of samples through plunge freezing is restricted to sample depths of about 10 μm and could lead to artefact formation and noisy data in areas that are only partially vitrified⁵⁰. Despite the merits which CLXT offers, cryopreservation also means that real-time-

lapsed imaging is not attainable. To document what happens at specific times during biological processes, disease progression, pathogenic infection or response to external/internal stimuli, we have to use cryo-fixation of biological samples at critical time points in order to map event progression in our samples and draw meaningful quantitative and qualitative information. Despite the fact that cryopreservation helps cushion the damaging ultrastructural effects from intense illumination and radiation doses, depending on the sensitivity of the sample to heat, exposure time or sample preparation flaws, devitrification and heat damage can occur while exposing samples to laser illumination (10-100 W/cm² laser power) or soft-X-rays²². Furthermore, if care is not taken, loading and unloading samples as well as moving across imaging platforms can potentially lead to crystal ice formation on the surface or throughout the sample. Finally, it is important to note that, because soft X-rays are easily absorbed in air²², the soft X-ray microscope works under high vacuum (<10⁻⁶ Torr) and samples need to be loaded and transferred under vacuum conditions and at cryogenic temperatures (~77 K). This is a process that requires training and expertise, so it is normally offered to users at synchrotron facilities.

Because nanoparticles are used as fiducial markers in our correlative workflow, there can be variability in preparation and dispersal. For instance, some nanoparticles do not distribute and disperse evenly during preparation and are captured as aggregates in the field of view during image acquisition. Without appropriate dispersal (in x, y and z), it is difficult to achieve high correlation accuracy with these clumps of nanoparticles. In addition, some fluorescent nanoparticles produce variable fluorescence signal which may be insufficient in some cases to achieve the desired cross registration and correlation.

Correlative experiments can be performed on a variety of set-ups. This protocol only discusses flat supports (more specifically: EM grids) as this is the type used at B24 and BL09-Mistral. While these are the most common, some set-ups have other requirements. Other cryoSXT beamlines have different sample holders, such as capillary tubes which still allow CLXT⁶² and, depending on the cell of interest such as cells in suspension, might be preferred. Therefore, this protocol should not be considered the standard CLXT, but rather the most common CLXT workflow. Finally, this work does not offer a unique overarching protocol suited to all possible biological samples, but rather offers a methodical user-friendly way to design tailor-made sample preparation based on the suitability of commercially available fiducials for successful high correlation accuracy of 3D imaging data acquired under cryogenic conditions using CLXT.

Expertise needed to implement the protocol

Our protocol assumes familiarity with cell handling and propagation pertinent to the research projects that intend to take advantage of new CLXT technology. Experience in cryo-preservation via plunge or high-pressure freezing will enable the fast consolidation of our methods in working local protocols. B24 (<https://www.diamond.ac.uk/Instruments/Biological-Cryo-Imaging/B24.html>) and BL09-Mistral (<https://www.cells.es/en/beamlines/bl09-mistral>) beamlines are part of Diamond Light Source and ALBA synchrotron facilities respectively. Hence, site access is subject to health and safety procedures and criteria fulfilments such as user training and compliance to local rules and regulations. New users of these facilities normally require support for the initial period of their visits by trained beamline staff before they are able to collect data independently. Sample preparation and cryopreservation training courses are offered regularly at both synchrotrons and aim to offer hands-on experience in applying the protocols described here. In addition to user support, user manuals are available to the community (onsite and online) and routine outreach activities ensure rapid dissemination of ongoing progress and development.

Experimental design

Requirements for fiducial markers. The need for fiducialisation can be met through commercially available materials such as non-fluorescent gold nanoparticles^{30,41}, fluorescent gold nanoparticles^{31,63}, silver nanoparticles^{64–66}, fluorescent microsphere beads (TetraSpeck and PS-Speck)^{67–69}, quantum dots (QDs)^{58,70,71}, fluorescent nanodiamonds⁷² and magnetic Dynabeads^{73,74}. Based on the data presented in this Protocol and factoring in the requirements of multimodal bioimaging, a fiducial is considered a candidate correlative tool in CLXT if: (a) it has fluorescence signal with high quantum yield (so it can be observed through excitation with visible light); (b) it absorbs X-rays in the ‘water window’ strongly (so that it can be easily identified); (c) it is of appropriate size (preferably between 100 – 250 nm) so as to be clearly visible in both modalities, and (d) be well dispersed throughout the sample (to ensure it is present in all possible regions of interest). Note that the Fresnel zone plate lens used in cryoSXT has a limited depth of field, and therefore the 3D reconstruction will not present an isotropic spatial resolution. In general, fiducials can be either on top of the sample support or on top of the cells, resulting in a difference in height of several microns. This can downgrade the achievable correlation accuracy depending on the cell type used (thick cells such as macrophages versus flat cells such as epithelial cells, for instance). With the right combination of fiducial markers, image correlation software such as eC-CLEM plug-in in ICY⁷⁵ or BigWarp plug-in in Fiji⁷⁶ can be used to scale and align 2D projections and 3D data volumes based on common features^{16,45,75} (**Supplementary Figure 1**).

Selecting commercial fiducials for direct comparison. We used representative cell populations and a range of candidate nanoparticles that are available commercially to devise the experimental approach presented here. We assessed the suitability of a number of compounds for our 3D correlative cryo-imaging approach (**Figure 2 and Supplementary Figures 2-5**) and amalgamated the resulting knowledge in a decision matrix (**Figure 3**) to allow the efficient use of single fiducials or combinations therein. ~~Several fiducialisation efforts have been reported previously (see following section).~~ An established approach in CLEM, now tested here in CLXT involves the conjugation of colloidal gold particles with fluorophores as a tool for correlation^{31,78,79}. Another effective correlative fiducial breakthrough involved the use of nanocomposite particles based on gold cores together with fluorescently labelled silica shells³¹. In this case, the gold core provided the needed contrast for electron microscopy (EM), while the fluorophores which were covalently integrated in the silica shell provided high quantum yields for fluorescence microscopy. Based on this and other reports^{31,63}, we opted to test the following fiducials. (**Supplementary Note 1** contains further information on all these reagents):

1) 150 nm DiagNano (AF488 and AF647, Creative Diagnostics, USA), a commercial fluorophore-labelled-gold nanoparticle in the size range needed for CLXT.

2) A similar approach based on silver (Ag) nanoparticles as the inner core but surrounded by silicon oxide (SiO₂) shells incorporated with fluorophores (Ursa BioScience)⁶⁴⁻⁶⁶. These silver nanoparticles are referred to as metal-enhanced fluorescence (MEF) nanoparticles, where sustained, bright and photostable fluorescence is enhanced significantly by synchronised tuning of the metal core and silica shell optical properties⁶⁴⁻⁶⁶. We selected Rhodamine B as the fluorophore of the MEF and chose fiducials with particle diameters of 200 and 250 nm in total (core + shell).

3) Fluorescent microspheres such as TetraSpecks^{68,69,80,81} (Thermo Fisher Scientific) and PS-Specks⁶⁷ (Thermo Fisher Scientific) are also useful correlative tools which have been used for correlating fluorescence and EM datasets⁸¹. These fluorescent microspheres additionally aid in multi-channel fluorescence image alignment following chromatic shift.

4) Fluorescent nanoparticles are supplied as size-specific suspensions where diamond nanocrystals within contain point defects (commonly nitrogen (N) atoms incorporated in either N-vacancy or N-Vacancy-N patterns in the crystalline lattice) giving rise to fluorescence upon irradiation fluorescence. Unlike other potential markers, these can be used as carbon-dense fiducials of substantial brightness that are impervious to bleaching effect. For our studies we selected suspensions of 140 nm average size (Adamas Nano) to allow the unambiguous identification of these particles in cryoSXT data.

5) Magnetic Dynabeads are routinely used for cell tracking and harvesting as well as for the *in vitro* delivery of biomaterials^{82,83}. They can be a few micrometres in diameter making them excellent positional markers for initial gross alignment of images although their size precludes them from assisting with fine alignment in the nanometre scale.

Organelle structures as fiducials. Apart from inert fiducials incorporated into samples prior to plunge freezing, fluorescently tagged distinct structures and organelles present in cells, can be used for data correlation purposes^{84,85}. Using organelle structure and features as fiducials is advantageous in that they do not obstruct native ultrastructure in the region of interest (ROI) as they are a biologically-relevant and inherent part of that ultrastructure⁸⁴. In addition, taking advantage of biological structures as fiducials means that the subject matter will be unperturbed by interaction with non-native material. This is particularly important for projects investigating the interaction of heavy metals with biological components and which might therefore be particularly sensitive to extraneous metal-based nanoparticles⁸⁶. Furthermore, the use of native fiducials as correlation tools means that, in addition to keeping samples as near-physiological as possible, we also minimise effort and time spent on other fiducials and their application. Following this line of reasoning, ubiquitous intracellular organelles, such as mitochondria, are potentially appealing correlation agents considering that they can be fluorescently labelled easily in live cells, they are ever present, and they are clearly visible through CLXT. However, mitochondria are large and polymorphic, and therefore may fail to deliver nanometre accurate 3D correlation. A biological candidate that can fulfil the necessary requirements for accurate high resolution correlation of heterologous data are lipid droplets⁸⁷ (**Figure 4**). These are broadly spherical and exist in abundance in most cell types. They can be preferentially labelled with targeted fluorescent dyes and are very absorbent in the 'water' window range (although their relative numbers, uneven distribution and heterogeneity in size and content can detract somewhat from their presumed efficacy).

Suitability of the different fiducial markers. We summarise here the suitability of the tested fiducials in terms of fluorescence and absorption signals. Fluorescent gold and silver nanoparticles as well as monovalent nanodiamonds (between 140 – 150 nm) have strong fluorescence signal and good X-ray absorption profile^{88,89}. Fluorescent microspheres (TetraSpeck) are made from carbon-based polymers that have weak X-ray absorption on 2D projections and 2D X-ray mosaics but, can be well resolved in the 3D reconstructed data sets provided the noise level in the specific ROI is low giving high correlation accuracy. Furthermore, organelle trackers such as mitochondria and lysosome trackers, as well as nuclear stain deliver excellent fluorescence signal making them ideal markers for cryoSIM. In parallel, these organelles are generally carbon-rich and have distinct and traceable structures following cryoSXT. Lipid droplets, which are heterogeneous in size and content, were also

enlisted as correlative tools due to their ability to be fluorescently labelled as well as their strong X-ray absorption contrast since they are carbon-rich organelles. Finally, magnetic beads (Dynabeads) are large (4.5 μm) in size and as a consequence are poor candidates for high correlation accuracy. They can serve as unmistakable gigantic landmarks in vitrified samples but their size preclude from having many of them well distributed and can unfortunately hide cells or structures below them as their absorption contrast is high⁹⁰. These data have been summarised in **Figure 2** and **Figure 4** as well as in **Supplementary Figures 2-5** where the efficiency of 3D registration for cryoSIM and cryoSXT is reported. Taken together, these observations will allow researchers to prepare samples and collect data that is amenable to *in silico* 3D alignment with clearly identified positional markers.

Materials

Biological materials

- U2OS cells (ATCC, Identifier ATCC HTB-96; RRID [CVCL_0042](#))
- HeLa cells (ATCC CCL-2; RRID [CVCL_0030](#); gifted from Maud Dumoux, from the Research Complex at Harwell, UK)
- NIH-3T3 cells (ATCC CLR-1658; RRID [CVCL_0594](#); gifted from Montserrat Romero from Institute for Research in Biomedicine Barcelona, Spain)
- *Drosophila melanogaster* primary post-embryonic haemocytes (plasmotocytes) from 3rd instar larvae (*Drosophila* strain Oregon^R, obtained from Bloomington Stock Center)
- Primary human CD8⁺ T cells - isolated by negative selection (RosetteSep Human CD8⁺ T cell Enrichment Cocktail, STEMCELL technologies, Cat#:15023) from anonymised leukopoiesis products from healthy donors acquired from the National Health Service blood service at Oxford University Hospitals under ethics licence REC 11/H0711/7

CAUTION All experiments involving human samples must be approved by an ethics committee in accordance with ethical guidelines of the institutional and national regulations. Informed consent has to be obtained from the involved individuals.

CAUTION It is recommended that cells be acquired from ATCC or through credible sources and collaborations and the number of passages be noted at all times. The cell lines used in your research should be regularly checked to ensure they are authentic and are not infected with mycoplasma

Reagents

- Dulbecco's Modified Eagle Media (DMEM; Thermo Fisher Scientific, Product code: 11590366)
- Fetal Bovine Serum (FBS; Capricorn, Cat#: FBS-11A)
- Bovine Serum Albumin (BSA; Sigma-Aldrich, SKU: A9418)
- L-Glutamine (Thermo Fisher Scientific, Cat#: 25030081)
- Penicillin/Streptomycin (10000 U/ml; Thermo Fisher Scientific, Cat#: 15070063)
- Hanks' Balanced Salt Solution (HBSS; Thermo Fisher Scientific, Cat#: 14175095)

- 457 • Trypsin-EDTA (0.25% (wt/vol)) (Thermo Fisher Scientific, Cat#: 25200056)
- 458 • Schneider's Drosophila medium (Thermo Fisher Scientific, Cat#: 21720024)
- 459 • RPMI 1640 (Thermo Fisher Scientific, Cat#: 31870074)
- 460 • HEPES (Thermo Fisher Scientific, Cat#: 15630080)
- 461 • Non-essential amino acids (Thermo Fisher Scientific, Cat#: 11140035)
- 462 • FBS; used to propagate primary human CD8⁺ T cells (Thermo Fisher Scientific, Cat#:
- 463 A3160801)
- 464 • IL-2 - Interleukin 2 (PeproTech, Cat#: 200-02)
- 465 • Tris (Melford Biolaboratories, Cat# B2005)
- 466 • NaCl (VWR, Cat#: 27810.364)
- 467 • HCl (Sigma-Aldrich, Cat# H1758)
- 468 • Dimethyl sulfoxide, anhydrous (DMSO; Thermo Fisher Scientific, Cat#: D12345)
- 469 • Poly-L-lysine (Sigma Cat# P4832)

470

471 ***Fluorescent reagents (nanoparticles and dyes)***

472 **CRITICAL** All fluorescent reagents used in this protocol have been obtained commercially.
 473 The description provided in this section might differ from the published protocols provided by
 474 the manufacturer. Before using any reagent, the original datasheet, available on distributor's
 475 website, should be consulted.

476 **CRITICAL** All fluorescent reagents should be shielded from exposure to white light during
 477 preparation and incubation as they are light sensitive.

478 **CRITICAL** All fluorescent reagents should be prepared from stock when needed and any
 479 material at working concentration should be discarded.

480

- 481 • Mitotracker Deep Red FM (Thermo Fisher Scientific, Product code:12010156)
- 482 • Mitotracker Green FM (Thermo Fisher Scientific, Product code:11589106)
- 483 • NucBlue Live ReadyProbes (Hoechst 33342; Thermo Fisher Scientific, Cat#: R37605)
- 484 • LysoTracker Red (Thermo Fisher Scientific, Product code:12090146)
- 485 • ER-Tracker Green (Thermo Fisher Scientific, Product code:11594746)

- 486 • LipidSpot 488 (Biotium, Cat#: 70065)
- 487 • LipidSpot 610 (Biotium, Cat#: 70069)
- 488 • TetraSpeck Microspheres (0.1 µm; Thermo Fisher Scientific (Invitrogen), Cat#: T7279)
- 489 • TetraSpeck Microspheres (0.2µm; Thermo Fisher Scientific (Invitrogen), Cat#: T7280)
- 490 • Fluorescent Gold Nanoparticles (AF488 and AF647 150 nm; Creative Diagnostics,
- 491 Cat#: GFL-150)
- 492 • Fluorescent Silver Nanoparticles (150 nm of Rh B Metal-Enhanced Fluorescence
- 493 Nanoparticles; Ursa BioScience, SKU: 170105)
- 494 • Carboxylated Green Fluorescent Nanodiamonds (140 nm; Adamas Nano, SKU:
- 495 NDNVN140nmMd10ml)
- 496 • Dynabeads Human T-Activator CD3/CD28 (4.5 µm; Thermo Fisher Scientific (Gibco),
- 497 Cat#:11131D)

498

499 ***Non-fluorescent fiducials***

- 500 • 250 nm gold nanoparticle fiducials (BBI Solutions, SKU: EM.GC250)
- 501 • 150 nm gold nanoparticle fiducials (BBI Solutions, SKU: EM.GC150)
- 502 • 100 nm gold nanoparticles fiducials (BBI Solutions, SKU: EM.GC100)

503

504 **Equipment**

- 505 • TEM Au grids (Quantifoil, Product code: AU G200F1 finder)
- 506 • PELCO easiGlow cryoEM glow discharge unit (Agar Scientific, Product code:
- 507 AGB7361)
- 508 • Cryo grid box (Agar Scientific, Product code: AG160-40W)
- 509 • Stereo microscope Stemi 2000 (Carl Zeiss)
- 510 • Primovert microscope (Carl Zeiss)
- 511 • Fisherbrand ultrasonic bath sonicator (Thermo Fisher Scientific, Cat#: FB11201)
- 512 • Plunge freezer (Leica Microsystems, Model: Leica EM GP)
- 513 • Cryo tool dryer (Leica Microsystems, Model: Leica EM CTD)
- 514 • Axiolmager microscope (Zeiss, Axio Imager 2)

- 515 • CryoSIM & AxioImager Linkam cryo-stages (Linkam Scientific, Cat#: CMS196M LED
- 516 Cryo Correlative Stage)
- 517 • CryoSIM microscope (Bespoke; B24 Diamond Light Source ²⁶⁾)
- 518 • TXRM microscope (Zeiss, UltraXRM-S220C)
- 519 **Software**
- 520 • Cockpit (Micron, <https://github.com/MicronOxford/cockpit>)
- 521 • SoftWoRx 6.5.2 (GE Healthcare)
- 522 [http://incelldownload.gehealthcare.com/bin/download_data/SoftWoRx/6.5.2/Soft](http://incelldownload.gehealthcare.com/bin/download_data/SoftWoRx/6.5.2/SoftWoRx.htm)
- 523 [WoRx.htm](http://incelldownload.gehealthcare.com/bin/download_data/SoftWoRx/6.5.2/SoftWoRx.htm))
- 524 • Chromagnon (<https://github.com/macronucleus/chromagnon> ⁹¹⁾)
- 525 • Fiji (<https://imagej.net/Fiji> ⁹²⁾)
- 526 • SIMcheck (<https://github.com/MicronOxford/SIMcheck> ⁹³⁾)
- 527 • TXRM Controller (Zeiss X-ray microscopy)
- 528 • IMOD package (version 4.9.2) (<https://bio3d.colorado.edu/imod/> ⁹⁴⁾)
- 529 • ICY (<https://icy.bioimageanalysis.org> ⁷⁷⁾)
- 530 • eC-CLEM plugin of ICY (<http://icy.bioimageanalysis.org/plugin/ec-CLEM> ⁷⁵⁾)
- 531 • SuRVoS (<https://diamondlightsource.github.io/SuRVoS/> ⁹⁵⁾)
- 532 • ChimeraX (<https://www.cgl.ucsf.edu/chimerax/> ⁹⁶⁾)
- 533 • TomoJ (ART)
- 534 (<https://bmcbioinformatics.biomedcentral.com/articles/10.1186/1471-2105-8-288>)
- 535 • Tomo3D (<https://sites.google.com/site/3demimageprocessing/tomo3d>)
- 536

Reagent setup

CRITICAL All reagents setup items should also be prepared under sterile conditions to avoid contamination and protect the lab personnel as well.

CRITICAL The nanoparticles described below are all stocked as suspensions and as such have a propensity for clumping leading to poor dispersal in the sample. All working suspensions need to be vortexed vigorously and for extended periods to ensure homogeneous dispersal. Two alternative protocols involving BSA coating and sonication respectively are offered in the Procedure section (Step 10).

CRITICAL If nanoparticles are not immediately used, they should be vortexed constantly until they are needed to ensure no sediment is formed that could promote aggregation.

CRITICAL If centrifugation is used to sediment nanoparticles, care should be taken to always use the lowest spin setting (~~100-200 RCF~~) (40-50 xg). Where possible suspensions should be allowed to sediment gradually during overnight storage at 4°C.

Tris-Buffered Saline Solution (TBSS, 0.9% (wt/vol))

Combine 6.05 g Tris, 8.76 g NaCl in 800 ml of ddH₂O. Adjust the pH to 7.4 with 1 M HCl and make volume up to 1 L with ddH₂O. This buffer can be stored at 21 °C for up to 6 months. Any isotonic buffered solution that will not adversely affect the target cell population can also substitute for TBS

Cells lines

Cell lines should be propagated in appropriate containment level I or II laboratories (ideally Class I or II biological safety cabinets should always be used). All cell lines used in this protocol should be maintained in DMEM containing 25 mM (4500 mg/L) D-Glucose, 1 mM (110 mg/L) sodium pyruvate, non-essential amino acids (NEAA) and supplemented with 10% (vol/vol) FBS, 4 mM L-Glutamine, 10% (vol/vol) Penicillin/Streptomycin (final concentration of 1000 U/ml) or similar ⁹⁷. The DMEM that is recommended uses a sodium bicarbonate buffer system (3.7 g/L), hence, it requires 5 – 10% CO₂ environment to maintain physiological pH. Complete cell culture medium can be stored at 4°C for up to 2 months.

569

570

571

572 **Drosophila primary plasmatocytes**

573 Drosophila primary plasmatocytes should be extracted in Drosophila Hemocyte Isolating
574 Medium (DHIM) containing 80% (vol/vol) Schneider's Drosophila medium supplemented with
575 20% (vol/vol) FBS as described in ⁹⁸. All reagents should be filtered-sterile and can be kept at
576 4°C for up to 2 months. Extracted cells should be used immediately.

577

578 **Human CD8+ T cells**

579 Primary human CD8+ T cells should be cultured in complete R10 medium (RPMI 1640, 10%
580 (vol/vol) FBS, 1% (vol/vol) Penicillin/Streptomycin, 1% (vol/vol) L-Glutamine, 1% (vol/vol) Non-
581 Essential amino acids and 25 mM HEPES) supplemented with 50 U/ml of recombinant IL-2 ⁹⁹.
582 Primary cells should be used as soon as they are isolated. Complete primary cell culture
583 medium can be stored at 4°C for up to 2 months.

584

585 **Non-fluorescent gold nanoparticles**

586 Non-fluorescent gold fiducials should be prepared fresh prior to cryofixation of samples. This
587 can be done by vortexing the stock nanoparticles solution for 1-2 minutes, before taking out 1
588 ml for preparation. To prepare ready-to-use nanoparticles, centrifuge at the lowest speed (40-
589 50 xg) for 15 minutes and then removing 970 µl of the cleared supernatant. The pellet should
590 be resuspended in 50 µl of serum-free culture media or similar and vortexed for efficient
591 dispersal continuously until it is ready to be used. Gold nanoparticles should be prepared fresh
592 but can be stored at 4°C overnight and vortexed to resuspend for at least 15 min before use. 2
593 µl of gold nanoparticles can be applied to each sample grid before blotting and vitrification
594 therefore, a 50 µl suspension will provide enough material to prepare up to 20 grids
595 (depending on transfer losses on container surfaces).

596

597 **CRITICAL** For CLXT experiments it is advisable to use 100 nm - 250 nm diameter gold beads
598 to ensure easy detection in cryoSXT that will allow automated processing with the least
599 obstruction of areas of the field of view.

CRITICAL Uniform dispersion of gold nanoparticles should be tested on a control sample containing the target biological material in its expected confluence on an EM grid. This can be done by applying 2 µl of the fiducials at working dilution to a hydrated populated grid (in the case of adherent cells this should be removed carefully from the culture environment using forceps) and blotting the extra liquid with filter paper on the side of the grid and away from the cells. The grid should then be inspected using conventional-light widefield imaging (ideally a microscope equipped with a 50X 0.55 DIC objective) for the presence of gold particle aggregation. If dispersal issues are identified, then either sonication or coating with BSA should be employed (**Figure 6**) as described in Step 10 of the 'Procedure' section.

ER-Tracker

Stock aliquots of ER-Trackers ¹⁰⁰ are prepared as 1 mM in DMSO (or in accordance to manufacturer specifications) and subsequently stored at -20°C for up to 6 months. For labelling, prepare 1 µM solutions by dilution (1:1000) of the stock solution in prewarmed (to match the temperature of the biological sample) serum-free cell media such as DMEM. Vortex the working solutions briefly and keep them in shaded containers before application to grids populated with adherent cells. For cells in suspension, trackers can be added from stock directly to the cell media.

LipidSpot

This lipid droplet tracker (LipidSpot) ¹⁰¹ is provided as 100× concentrated solution in DMSO and stored at 4°C. Prepare the working solution via 1:100 dilution in prewarmed (to match the temperature of the biological sample) serum-free cell media such as DMEM. Vortex briefly to mix and use the mixture to replace the sample medium for labelling purposes. The working solutions can be stored at 20°C for up to 1 month.

Lysotracker

Prepare stock aliquots of LysoTracker¹⁰² as 1 mM in DMSO (or in accordance to manufacturer specifications). The aliquots can be stored at -20°C for up to 6 months. For labelling, prepare 0.05 µM solutions by dilution (1:20,000) of the stock solution in prewarmed (to match the temperature of the biological sample) serum-free cell media such as DMEM; we recommend preparing working solution through a series of dilutions to ensure accuracy. Vortex the working solutions briefly and keep them in shaded containers before application to grids populated with adherent cells. For cells in suspension, trackers can be added from stock directly to the cell media. The working solutions can be stored at 20°C for up to 1 month.

Mitotracker

Prepare stock aliquots of Mitotracker¹⁰³ as 1 mM in DMSO (or in accordance to manufacturer specifications). The aliquots can be stored at -20°C for up to 6 months. For labelling, prepare 0.1 µM solutions by dilution (1:10,000) of the stock solution in prewarmed (to match the temperature of the biological sample) serum-free cell media such as DMEM; we recommend preparing working solution through a series of dilutions to ensure accuracy. Vortex the working solutions briefly and keep them in shaded containers before application to grids populated with adherent cells. For cells in suspension, trackers can be added from stock directly to the cell media. The working solutions can be stored at -20°C for up to 1 month.

NucBlue Live ReadyProbes

Prepare the working labelling solution by adding 2 drops of NucBlue nuclear stain¹⁰⁴ (supplied by the manufacturer as a 40.6 µM solution in water) to each ml of serum-free media such as DMEM at the temperature required for cell maintenance. The working labelling solution should be used within 30 minutes of preparation and cannot be stored long term.

CRITICAL ~~Timing is of the essence while tracking organelles with membrane-permeable fluorescent dyes as they are gradually disposed of and recycled within target cells.~~

Fluorescent microspheres (TetraSpeck)

Prepare microsphere stock suspensions (provided by the manufacturer as 10¹⁰-10¹¹ particles/ml in dH₂O/2 nM sodium azide) as a 1:10 dilution in serum-free culture media prior to use; this relatively concentrated working suspension will ensure the presence of a critical mass of fiducials that can be identified in both cryoSIM and cryoSXT. Prepared microspheres can be

stored for up to a week at 4°C provided they are shielded from exposure to light (microcentrifuge tubes and containers should be covered with aluminium foil or similar).

Fluorescent gold (Au) nanoparticles

Prepare stock suspensions of gold nanoparticles (provided by the manufacturer as 7E+10 particles /ml in dH₂O/2 nM sodium azide) as a 1:10 dilution in serum-free culture media or suitably buffered isotonic solutions before used for fiducialisation by addition of 2 µl directly onto sample grids prior to blotting and plunge-freezing (Procedure section, Step 27). Prepared gold nanoparticles can be stored for up to a week at 4°C provided they are shielded from exposure to light (microcentrifuge tubes and containers should be covered with aluminium foil or similar).

Fluorescent silver (MEF: Metal Enhanced Fluorescence) nanoparticles

Prepare fluorescent silver nanoparticles (provided by the manufacturer in powder form and resuspended in 1ml of serum-free media to 0.25 mg/ml stock concentration and stored at 4°C) as a 1:100 dilution in serum-free culture media or suitably buffered isotonic solutions before used for fiducialisation by addition of 2 µl directly onto sample grids prior to blotting and plunge-freezing (Procedure, Step 27). MEF nanoparticles should be prepared to the desired quantity. immediately before use (storage of the suspension is not recommended).

CRITICAL ~~If nanoparticles are not immediately used, they should be vortexed constantly until they are needed to ensure no sediment is formed that could promote aggregation.~~

Fluorescent nanodiamonds (FNDs)

Commercial suspensions of fluorescent nanodiamonds (commonly provided by manufacturers as suspensions of particles with variable size) are buffer exchanged to produce 1x stock solutions. To do this add 1ml of the suspension in a microcentrifuge tube and centrifuge at lowest setting available (typically 40-50 xg) for 10 minutes at room temperature (18-23°C). Carefully aspirate the supernatant and resuspend in 100 µl of serum-free culture media. Keep the working suspension on vortex until needed. FNDs can be prepared in advance and stored long term at 4°C provided they are contained in sterile media.

696 **Magnetic beads (Dynabeads)**

697 Prepare dynabeads as a 4×10^7 beads/ml in phosphate buffer saline (PBS), pH 7.4. Prior to
698 use, vortex the beads briefly to ensure homogenous suspension. Beads are compatible with
699 cell culture media and can be prepared at 1:100 to 1:1000 dilution prior to plunge-freezing. No
700 extensive vortexing is required prior to use as they display little to no propensity towards
701 clumping. Dynabeads can be prepared a day in advance and kept at 4°C for several weeks.

702

703

Equipment setup

Tissue culture and vitrification

To protect laboratory users and ensure contamination-free sample preparation, tissue culture and vitrification (plunge-freezing and high-pressure freezing) apparatus should ideally be housed in biosafety level II rooms.

CryoSIM and cryoSXT

To limit the impact of humidity and temperature fluctuations on vitrification, stability of cryopreserved samples, sample loading as well as ensure the success of cryoSIM and cryoSXT imaging sessions, equipment should ideally be housed in temperature and humidity-controlled areas or enclosures.

Procedure

CRITICAL A flowchart showing a graphical representation of the CLXT correlative workflow is shown in **Figure 1**.

Preparation of sample grids

1) Quantifoil TEM grids (AU G200F1 or similar) ¹ are hydrophobic, hence they need to be treated before use in order to be easily submerged in media without floating and in order for cells or tissue to comfortably attach to them. There are various ways to achieve this and here, we present the three alternatives which we commonly use. To glow/plasma discharge using the easiGlow unit, follow Option A. Another means of hydrophilizing grids is by pre-coating them in FBS 6 – 24 h before cells are seeded on them. To do this, follow Option B. For coating grids with poly-L-lysine, follow Option C

TROUBLESHOOTING

CRITICAL Grids can be easily damaged so should always be handled cautiously from the rim and with precision (occasionally denoted as surgical) fine tip tweezers. Self-closing inverted

tweezers are recommended if prolonged handling is anticipated as they require no force to remain closed.

CRITICAL When lifting a grid, forceps should hold the grid from the rim and their tips should not extend far into the stamped central area to avoid mechanical damage to the fragile support film. Ideally, a set of forceps is kept solely for the purposes of sample grid manipulations and their tips are regularly inspected for distortions that could damage the surface of the TEM grid.

CRITICAL All grid handling should be carried within an aseptic environment such as a BSL-2 laminar flow cabinet; forceps should be regularly rinsed with 70% ethanol solution and left to air dry as often as possible.

CRITICAL The use of finder grids (TEM grids stamped with positional markers) is highly encouraged as they allow unambiguous mapping and ease identification and recovery of area-of-interest coordinates across microscopes.

A) Glow/plasma discharge Timing 15 minutes

CRITICAL Instructions included pertain to the easiGlow discharge unit¹⁰⁵ but can accordingly be adapted to other glow discharge units dependent on specification¹⁰⁵

CRITICAL A glow discharge unit (**Figure 5a-e**) can be used for hydrophilization and cleaning of TEM grids and carbon-based sample support films.

i) Place grids (carbon film side up) on a parafilm-wrapped glass slide and position the slide in the designated sample stand in the discharge unit.

ii) Cover the glow discharge head with its glass cover to isolate the area that will be placed under vacuum.

iii) Turn on the main power to the unit. When this is done, the easiGlow touch panel will display the AUTO RUN screen (alongside manual setup menus). Glow discharge units commonly offer automatic modes for easy use.

iv) Select auto mode by pressing “AUTO RUN” on the touch panel (suggested actions include: pump to 0.4 mBar; hold 10 seconds; glow discharge 25 seconds at 15 mA negative polarity; slow vent to atmosphere).

v) Retrieve grids once plasma discharge is completed and the chamber has returned to atmospheric pressure (the lid can now safely be removed).

CRITICAL STEP If using a re-enforced glass cover for the vacuum chamber ensure pressure has reached atmosphere values (1010 mBar; 760 Torr) before attempting to remove the lid and recover grids.

PAUSE POINT

Glow discharged grids will retain surface charge and associated hydrophilicity for 30 min-3 h depending on ambient humidity levels.

B) Coating grids in serum Timing 8-16 hours

- i) Using forceps, gently pick up a grid being careful not to bend it or disrupt the carbon-support film. Inverted forceps will provide extra hold stability as they do not require constant pressure by the operator but do require familiarity with their use.
- ii) Briefly dip the grid in 70% ethanol.
- iii) Rinse off excess alcohol by dipping into sterile HBSS.
- iv) Submerge the grids in 0.5-1 ml of filtered-sterilised FBS and hold them under the surface before releasing them from the forceps, ensuring the carbon support side is facing up when the grids rest at the bottom of the container (commonly a well in a 6-well culture plate).
- v) Incubate at 21-37°C overnight. Culture trays containing grids can be incubated alongside cell cultures in any standard non-shaking incubator.
- vi) Gently aspirate the FBS and further wash with 1 ml HBSS before aspirating again.
- vii) Add enough HBSS (or an appropriate buffered isotonic solution) to keep the grids submerged.

PAUSE POINT

Serum-coated grids should ideally be used immediately but can be stored at room temperature for up to 2 h.

C) Coating grids with poly-L-lysine. Timing 30 minutes

CRITICAL The procedure presented here is optimised for coating with poly-L-lysine^{106,107} but can be adapted for using similarly charged amino acid solutions such as poly-ornithine

~~**CRITICAL** Metal grids and support films can also be charged further using charged amino acids. To do this repeat steps A (i)-(v) or in the absence of a glow discharge unit steps B (i)-(iii).~~

- 797 i) Using forceps gently retrieve grids and place in filtered 0.01% poly-L-lysine solution.
798 ii) Incubate at room temperature for 10-30 minutes.
799 iii) Carefully aspirate the solution and rinse with 1 ml HBSS.

800 **PAUSE POINT**

801 Poly-L-lysine coated grids can be stored in HBSS at 4°C for up to 24 h. Equilibrate to room
802 temperature before use.

803

804 **Seeding of cells on grids**

805 2) Seed the cells onto the grids. When using immortalised cell lines, follow Option A. When
806 using plasmacytes extracted from *Drosophila melanogaster*, follow Option B. When using
807 cells/samples in suspension (e.g. primary human CD8⁺ T cells), follow Option C.

808 **A) Immortalised cell lines** **Timing 24-48 hours:**

- 809 i) Culture cells according to established protocols. Ideally, cultures should be allowed to
810 reach high density to ensure that sufficient numbers are present for seeding on grids.

811 **CRITICAL STEP** It is important to passage cultured cells at least once from stock to ensure
812 viability but avoid double digit passages that have aged and could develop differently than
813 stock cells.

- 814 ii) Detach cells following established protocols (these depend on the demands of the
815 particular cell line and project; gentle trypsinization is commonly used to lift and harvest
816 adherent cells) and concentrate to $>1 \times 10^6$ cells/ml in complete primary cell culture
817 medium.

- 818 iii) Dispense small volumes of cell suspension in the containers that will be used for seeding
819 on grids (typically 6-well tissue culture plates or multi-chambered slides). As a guide, a 1
820 ml 5×10^4 cell/ml suspension of U2OS cells in a single well of a typical 6-well culture tray
821 will result in 40-50% adherent-cell coverage on a 3mm TEM grid after 24 h incubation at
822 37°C with 5% CO₂).

823 **CRITICAL STEP** The choice of container should be leveraged against forceps access
824 requirements. Remember that grids need to be gently deposited in sample-containing wells
825 and recovered from them later without damaging their structure or that of their carbon-support.
826 If sharp-tip forceps cannot comfortably lift and capture a grid it is likely that they will apply
827 excessive mechanical force and bend or rupture it.

- iv) Using inverted forceps, add prepared grids (Step 1) to the cell cultures containers (6-well culture trays can accommodate 1-5 grids each).
- v) Monitor cell attachment and growth at regular intervals (12 h, 24 h or similar) with a conventional light microscope until they are sufficiently confluent. Unless a given cell density is required for experimental purposes, a confluency of 60-80% will ensure both sample abundance for imaging and sample resilience during blotting.

TROUBLESHOOTING

CRITICAL STEP If grid surfaces are over-populated (high confluency of multi-layering) the sample will not be blotted efficiently and is likely to be unsuitable for cryo-imaging.

B) Plasmotocytes extraction from *Drosophila melanogaster* **Timing 3 hours:**

- ii) Add 0.1-0.5 ml of the DHIM medium in a dissection well and use inverted forceps to submerge into it a prepared grid (Step 1).
- ii) Extract *Drosophila* post-embryonic haemocytes (plasmotocytes) from 3rd instar *Drosophila* larvae according to established protocols¹⁰⁸ (3-5 larvae per grid required) in the dissection well and over the grid resting at its bottom.
- iii) Allow the cells to settle on the grid surface for 45 mins at RT.
- iv) Monitor cell settlement on grids with a conventional light microscope (30 min-1 h).

CRITICAL STEP Inspect the grids after the dissection of each individual until desired cell density is achieved.

C) Cells/samples in suspension (e.g. primary human CD8⁺ T cells) **Timing 10 minutes**

CRITICAL Cells in suspension and other particulate samples can be deposited on grids prior to plunge freezing (a 3 mm TEM grid can mechanically hold on its surface a maximum of 2 µl of a standard non-detergent containing culture medium). The user should decide on the volume to add given the density of the sample suspension at hand and the desired density on grids per project. If there is a call to fluorescently label organelles within such samples, steps 3 –7 should be performed before the deposition, with the exception that fluorophores can be

added directly to the suspension. When the cells in solution are ready for deposition the following steps are involved:

- i) Use inverted forceps to pick a prepared grid (Step 1) and rest them on a flat surface with the grid carbon film surface facing upwards.
- ii) Add up to 2 μ l of cells in suspension (20-300 cells in total depending on size) on the surface of the grid and allow them to settle for about 1 minute.

CRITICAL STEP The density of sample suspension (total number of cells per μ l) added to a 3 mm TEM grid should be calculated to produce grid surface coverage of 60-80% after blotting (the total number of cells given the volume deposited on the grid).

CRITICAL STEP Samples maintained in high salt buffers should be deposited on grids and blotted either as rapidly as possible or within a temperature-controlled humidified chamber (room temperature at 80% humidity) to avoid dehydration that can lead to crystalline salt formation in the solution.

- iii) Monitor cell settling with a conventional light microscope. A surface coverage of 60-80% will ensure both sample abundance for imaging and sample resilience during blotting.

(Optional) Fluorescent labelling of organelles **Timing 20-30 minutes**

CRITICAL Samples ready for cryopreservation can be fluorescently labelled up to 30 minutes prior to plunge freezing. To achieve efficient fluorescent labelling, the Steps 3-8 are involved:

- 3) Thaw stock fluorescent trackers and allow to reach room temperature.

CRITICAL STEP Fluorescent dyes should be shielded from light during preparation and incubation steps as they can be light sensitive.

CRITICAL STEP If samples are likely to be affected by temperature changes in their media, trackers can be warmed up before addition but prolonged incubation above RT could damage them (follow manufacturer's recommendations).

CRITICAL STEP Ensure that the application of any of the fluorophores used will not interfere with your experiment. For example, Mitotracker reacts with thiol groups and can interfere with mitochondrial membrane potential and ion shuttling.

4) Dilute the required organelle tracker dye(s) to a volume of culture medium that just supersedes requirements. For example, if three wells of a 6-well tray are occupied with grids they will require 0.5 ml of medium per well to ensure uniform coverage with the minimal expenditure of trackers; in this case, 3×0.5 ml (absolute requirement) + 0.5 ml (safety excess) of medium should be prepared.

CRITICAL STEP Trackers that are used at very low concentrations such as LysoTracker require multi-step serial dilutions to minimise measuring errors and losses in pipette tips and should be diluted to a useful concentration at this point (a dye supplied as 1 mM stock that works as a 1:20000 dilution of 50 nM is best diluted from stock 1:20 and then 1:1000 to ensure all qualities can be reliably dispensed by standard plunger-based pipettes).

CRITICAL STEP Fluorescent dyes can also be added directly to the culture media in the wells containing sample grids and mixed in situ with gentle pipetting, but this should ideally be avoided as it can result in uneven dispersion or even induce morphological changes in susceptible cell populations due to sheer forces during pipetting. Alternatively, the whole plate can be gently tilted a couple of times in order to mix the media.

CRITICAL STEP Ensure that the incubation times required for different trackers are compatible (see Step 7) before preparing a 'cocktail'. If incubation times are drastically different then each tracker should be prepared separately and added to the samples so as the final required volume remains unchanged (if 0.5 ml of medium is required to keep grids submerged and two separate dyes are needed then 0.25 ml of each should be prepared to double the working concentration and added to the sample grids).

5) Bring samples (~~typically prepared grids with adherent cells in supplemented tissue culture media kept in 6 well culture trays or similar~~) to a biological safety laminar flow cabinet and position on a heated pad (temperature should agree with standard growth conditions).

CRITICAL STEP Move cultured cells gently avoiding shaking as much as possible to reduce mechanical forces that could induce shearing and morphological changes.

6) Carefully aspirate culture medium and add the formulation prepared in Step 4.

CRITICAL Timing is of the essence while tracking organelles with membrane-permeable fluorescent dyes as they are gradually disposed of and recycled within target cells.

7) Incubate at 37°C with 5% CO₂ or according to manufacturer's recommendations. For the membrane-permeable trackers included in our 'reagents' section we recommend incubation times of: ER-tracker 20-30 min, LipidSpot 20 min, LysoTracker 20 min, Mitotracker 10-15 min and NuBlue Live 20-30 min.

TROUBLESHOOTING

CRITICAL STEP Carefully review manufacturers recommendations on incubation time and temperature required to ensure successful labelling. Some dyes are recycled rapidly and for those all timings up to plunge-freezing should be considered towards the sum of the incubation period.

8) Cover the tissue culture plates with aluminium foil to prevent exposing fluorophores to white light interaction and incubate as specified in Step 7.

CRITICAL STEP Uptake of fluorescent dyes will depend on cell and sample type, temperature and culture growth state. In general, manufacturer's recommendations should be adhered to unless otherwise necessary because of specific sample requirements.

CRITICAL STEP Ideally, tracker uptake should be tested in advance in the target cell line at the required density using recommended protocols and conventional fluorescence imaging to

952 confirm temporal and spatial uptake in a new sample and intensity of fluorophore in the given
953 media and sample.

954 **CRITICAL STEP** While fluorescent dyes are being incorporated into the biological samples,
955 vitrification equipment and fiducials should be available and ready to use to prevent any delays
956 after the prescribed incubation time has elapsed.

957

958 9) At the end of the incubation period, inspect all grids under a conventional microscope for
959 confluency and cell morphology and vetted for further use.

960 **CRITICAL STEP** It is not necessary to wash away excess trackers after incubation because
961 blotting (Step 27) will remove excess solution. However, if the fluorescence signal expected is
962 weak, it is recommended that a final wash with warm serum-free culture medium will aid in the
963 removal of excess unbound fluorophore around and on top of cells.

964

965 **(Optional) Non-fluorescent gold nanoparticle dispersal optimization**

966

967 10) Fiducials should be prepared as described in the Reagent Setup. Alternate preparations
968 include sonication and BSA coating (**Figure 6**).

969

970 **CRITICAL** All solutions and reagents must be brought to a culture-appropriate temperature
971 before they are applied directly on samples.

972

973 **A) Sonication Timing ... 20 min with overnight incubation**

974 i) Add 1 ml of the nanoparticle stock suspension to a microcentrifuge tube and leave at 4°C
975 overnight to settle.

976 iii) Gently aspirate 0.97 ml of the supernatant without disturbing the settled nanobeads.

977 iv) Add 30 µl of 0.9% w/v RT TBS solution (see Reagent Setup) or equivalent and resuspend
978 by vortexing.

979 v) Fill the sonicator bath with ddH₂O and ice (aiming for a constant temperature range of 4-
980 10 °C during the sonication process).

981 vi) Sonicate the resuspended nanoparticles at 60-80 kHz (100% power) continuously for 10-
982 15 min and set module to pulse thereafter (pulses should include resting periods of 10-30

sec to avoid overheating). The fiducials should be kept sonicating until needed and placed back in the sonicator when not in use.

CRITICAL STEP Sonicator settings might need to be adjusted depending on the available model and output a user has access to. The temperature in the water bath should remain < 21°C at all times to ensure the suspension is not overheated and therefore a closely monitor shutter-proof thermometer should be inserted in the water bath and kept under watch.

vii) Remove microcentrifuge tube from sonicator and place it for 30-60 sec in a heated block or other heated surface (set to cell culture appropriate temperature) to avoid cell temperature shock upon nanoparticles addition.

viii) Vortex briefly before addition to sample grid in Step 27.

TROUBLESHOOTING

B) BSA coating **Timing ...45 min with overnight incubation**

CRITICAL Gold nanoparticles are usually deep orange in colour (the smaller the diameter, the darker the suspension appears); this colour can darken during incubation with BSA but this does not affect their distribution and application.

i) Add 1 ml of the nanoparticle stock suspension to a microcentrifuge tube and leave at 4°C overnight to settle.

ii) Prepare 10% (wt/vol) BSA in ddH₂O.

iii) Gently aspirate 0.97 ml of the supernatant from Step i without disturbing the nanobead pellet.

iv) Add 200-500 µl of filtered 10% (wt/vol) BSA, vortex for 20-30 minutes.

v) Centrifuge at ~~200 RCF~~ 40-50 xg for 30 min at room temperature.

vi) Gently aspirate supernatant and resuspend in 40 µl of the appropriate serum-free cell culture media. Mix by pipetting up and down.

v) Vortex the suspension continuously until needed in Step 27.

1013 TROUBLESHOOTING

1014

1015

1016 Fiducial addition and plunge freezing **Timing** 5-10 minutes

1017 **CRITICAL** Steps 11-32 effectively describe three intertwined processes: the preparation for
1018 plunging (Steps 11-26), the addition of prepared nanoparticles (Step 27), the blotting and the
1019 vitrification of the sample by plunge-freezing (Steps 28-33) into liquid nitrogen-cooled liquid
1020 ethane using in this case a Leica GP2 plunge freezer (**Figure 5h-m**).

1021 **CRITICAL** The procedure can be adapted by the reader for use of homemade plunge freezing
1022 modules as well as equivalent commercial equipment and was informed by previous work
1023 ^{109,110}.

1024

1025

1026 **CAUTION** Wear appropriate protective equipment during any steps involving cryogenic liquids,
1027 including clear wrap-around eye shield/goggles and/or polycarbonate face shield, non-
1028 allergenic nitrile gloves (cryogenic gloves are not recommended for fine manipulation of grid-
1029 based samples in cryogenic liquids) and long-sleeved laboratory coats.

1030

1031 11) Turn on the plunge-freezer (usually through a flick switch at the back of the module) and
1032 confirm start-up at the control touch screen.

1033 12) Insert container for liquid ethane into the heated holder.

1034 13) On the touch screen panel, set the liquid nitrogen tank temperature to -160°C.

1035 **CRITICAL STEP** The temperature of the ethane holder will increase once the ethane delivery
1036 cap is introduced. The user should wait until the temperature returns to -160°C before
1037 proceeding.

1038 14) Fill the cryogen chamber with liquid nitrogen to 75-100%.

1039 **CRITICAL STEP** When filling the liquid nitrogen tank for the first time, do so slowly and pause
1040 frequently to allow violent boil off. If this operation is done quickly the percentage fill value in
1041 the display will not accurate and the user can flood the sample area and all heaters
1042 underneath.

1043 15) Carefully load 60ml of distilled water into the humidity chamber using a syringe.

CRITICAL STEP A humidity chamber ensures that there is no loss of sample volume due to evaporation in the period before plunging. Should this module not be available all operations leading to vitrification should be done in an expedient but safe way to ensure not sample media evaporation that could change media concentration and stress residing cells.

16) Add blotting paper on the side holder and secure in place with metal shield or other fastening provided.

17) Use a test grid to ensure alignment for optimal blotting (load grid→lower chamber→select 'setup'→select 'blot position'→evaluate→select 'prepare' option).

CRITICAL STEP Blotting position (sample forceps tip contact with filter paper and alignment with cryogen pool should ideally be tested and adjusted ahead of time to ensure expediency.

18) Select 'load forceps' to elevate the humidity chamber.

19) Place the ethane delivery cap on top of the ethane receptacle (Step 12).

20) Once the temperature of the ethane vial and delivery cap reaches -160°C start slowly delivering gaseous ethane. If using a three-valve regulator fitted ethane bottle: open the valve on the ethane bottle completely and then open the intermediate valve gently until the outer most gauge reaches 1 psi (that is the pressure gaseous ethane will be delivered at). Gradually open the third valve on the ethane bottle while observing ethane condensation in the cryogen pot. Close all valves securely once the cryogen pot is visibly full.

CAUTION Ethane is a combustive agent and should be kept away from sparks or open flames.

CRITICAL STEP Before dispensing ethane through a multi-valve regulator ensure that all gauges other than the one most proximal to the gas cylinder register no pressure and all the valves are closed (the one on the gas cylinder could be open if the first gauge reads a value above zero).

CRITICAL STEP While delivering liquid ethane, the receiving pot will be first filled with condensed droplet and viewing can be obscured. This will however dissipate, and a meniscus will become obvious which will give rise to a flat surface as the level reaches the top of the pot.

CRITICAL STEP As gaseous ethane is delivered at room temperature and condenses upon contact with the cooled vial it is possible that the overall temperature of the module will

1076 increase enough to hinder further condensation. In that case, pause delivery until the required
1077 temperature is reached and resume.

1078 **CRITICAL STEP** To leave the ethane cylinder ready for use, close the main valve nearest the
1079 bottle and drain the gas from all other sections before closing all other valves.

1080 **CRITICAL STEP** If liquid nitrogen is accidentally introduced to the liquid ethane pot, the ethane
1081 inside it will freeze. If the pot is allowed to reach -160°C again the ethane will liquify again.

1082 21) Remove the lid from the ethane cylinder and close all valves on the ethane cylinder.

1083 22) Cover the ethane pot with a lid (to protect it from accidental exposure to liquid nitrogen)
1084 and top up the cooling chamber to 100% with liquid nitrogen.

1085

1086

1087 23) Remove the ethane pot lid and place a grid storage box inside the area designated for grid
1088 transfer post vitrification.

1089 **CRITICAL STEP** Before adding a sample storage box to the working area ensure it is
1090 appropriately labelled and the lid is loosely attached to allow ease of sample storage.

1091 24) Using the touch control screen set liquid nitrogen tank temperature to -170°C, humidity
1092 levels to 70-80% (if applicable).

1093 25) Select “program check” option and set the blotting time to 0.5-3 sec depending on cell
1094 confluence and cell/tissue type.

1095

1096 **TROUBLESHOOTING**

1097

1098

1099 26) Pick a sample grid (from Step 2 or 9) with the designated forceps that fit your plunge
1100 freezer and attach to the plunger module (in the Leica GP, the upper portion of the forceps’
1101 adaptor slides through a cut groove on the plunger arm).

1102 **CRITICAL STEP** Immediately prior to plunge freezing of samples, it is necessary to visually
1103 inspect cells on grids using a conventional light microscope for a final assessment of cell
1104 health and density and only grids optimally populated should proceed to vitrification.

1105 **CRITICAL STEP** Ideally, with cells at 40-60% confluency, 0.5 sec blotting time is enough to
1106 remove excess fluid while retaining 3D cell morphology. In the same vein, short blotting times

1107 of 0.5 sec may not be suitable for some cell types as this may yield non-uniform blotting
1108 leading to thick vitreous ice formation.

1109 **CRITICAL STEP** Tissue culture plates containing cells on grids should be kept on a heated
1110 surface (to culture requirements) away from vibrations on the run up to plunge freezing as this
1111 ensures that the absolute minimal amount of stress is impacted.

1112 **CRITICAL STEP** Once the sample grids are picked up with forceps in the tissue culture plates,
1113 it is important to drain them lightly by bringing them to the surface of the media and holding
1114 them just touching the liquid surface for a couple of seconds prior to loading them on the
1115 plunge freezer. This way, excess media trapped in the tweezer tips can be drained to ensure
1116 no ice forms there which might hinder release of the grid to its storage area in liquid nitrogen.

1117 **CRITICAL STEP** Pay attention to the position of the forceps. If using a one-sided blotting
1118 setup, the carbon side of the grid holding the cells should face away from the blotting paper to
1119 ensure no mechanical damage of the support film and the cells that reside on it.

1120 **CRITICAL STEP** Ensure that the protective lid has been removed from the ethane pot before
1121 plunging.

1122

1123 27) Lower the humidity chamber, add 1-2 μ l of prepared nanoparticles (assessed as described
1124 in 'Reagents preparation') through the appropriate access port on the side of the equipment
1125 and select 'Blot' on the touch screen.

1126

1127 **CRITICAL STEP** When dispensing nanoparticles directly on the grid surface (see Step 27),
1128 ensure that the pipette tip is close to the surface but not touching it. Only the suspension itself
1129 should come in contact with the surface of the grid to avoid mechanical damage.

1130 **CRITICAL STEP** Always look at the grids when blotting and ensure you can see liquid drawn
1131 out of the sample. If automated blotting has failed, you can attempt manual blotting with a
1132 small piece of filter paper which can be used to lightly wick media from the carbon film-free of
1133 the grid.

1134 **CRITICAL STEP** It may be important to alternate between blot times used in replicate grids.
1135 You should aim for the least amount of blotting that will remove excess media from the vicinity
1136 of the cells without flattening them. As a guide, a 60-70% confluent 3mm grid requires 0.5 sec
1137 of blotting given an average media formulation.

1138

1139 28) On the touch pad control screen select 'Plunge'.

1140 **CRITICAL STEP** Liquid nitrogen that will come into contact with samples should be filtered to
1141 ensure all crystalline ice has been removed. Crystalline ice deposited on grid surfaces through
1142 exposure to, or storage in, unclean cryogenic liquids is difficult to remove and will negatively
1143 impact CLXT data quality.

1144 29) Gently remove the sample forceps from the holding rod and transfer the grid from the
1145 ethane to the liquid nitrogen chamber.

1146 **TROUBLESHOOTING**

1147

1148 **CRITICAL STEP** Keep your eyes on the grid while transferring and ensure it remains
1149 submerged in cryogen at all times bar the brief and rapid transfer from ethane to nitrogen.

1150 **CRITICAL STEP** Before transferring from the liquid ethane, hold the grid above but just
1151 touching the cryogen surface for 1 to 2 seconds. This will ensure that extra ethane drains
1152 away and will minimise ethane ice on the sample once it is in liquid nitrogen.

1153

1154 30) Place the grid in the prepared storage box under liquid nitrogen and proceed to the next
1155 sample by following Steps 24-30 if needed.

1156

1157 **TROUBLESHOOTING**

1158

1159 **CRITICAL STEP** It is important for the forceps to be at a temperature that matches the
1160 maintenance temperature required by the sample material (room temperature is also adequate
1161 for the majority of cultured cell populations) before using them to pick up a sample grid for
1162 plunge freezing to prevent temperature shock. This is particularly important when re-using
1163 forceps after they are used to move samples within a cryogenic liquid; moreover, heating up
1164 the forceps to room temperature and beyond facilitates drying and removal of excess moisture
1165 that might otherwise lead to crystalline ice formation upon plunge freezing.

1166

1167

1168 31) At the end of sample preparation, carefully remove the ethane container and allow to
1169 evaporate at room temperature in a well-ventilated area. Remove the blotting paper and

dispose, drain the ddH₂O from the humidity chamber (if applicable) and select 'bake out' on the touch screen (repeat when prompted and leave the chamber door open). For a Leica GP, the bake out process commences after the liquid nitrogen in the storage dewar evaporates and takes 60 minutes; once completed the humidity chamber returns to its start-up position.

PAUSE POINT Grid boxes can be stored in a cryogen filled storage dewar (long term storage).

Cryo sample evaluation Timing 10-30 minutes

CRITICAL Access to a conventional visible light microscope equipped with a cryo-stage is required to evaluate cryopreserved samples on grids for CLXT. For a representative cryo-microscopy setup (a Zeiss AxioImager2 coupled to a Linkam cryo-stage in this instance), the following steps should be taken (**Figure 7a-c**):

32) Switch on the microscope and its light source.

33) Top-up the external liquid nitrogen dewar to two-third its capacity with liquid nitrogen and secure the vessel with the transparent lid.

CRITICAL STEP The stage and microscope should never be left unattended when they contain liquid nitrogen cooled samples.

CAUTION Wear appropriate protective equipment during the whole process including clear wrap-around eye shield/goggles and/or polycarbonate face shield, non-allergenic nitrile gloves (cryogenic gloves are not recommended for fine manipulation of grid-based samples in cryogenic liquids) and long sleeve laboratory coats.

CRITICAL STEP Before filling the external dewar ensure that the O-ring seal that contact the lid is properly fitted.

CRITICAL STEP Fill the external cryogen dewar slowly and pause frequently to ensure you avoid excessive boil off. Only fit the lid once the dewar is filled and the surface of the cryogen appear calm. Expect nitrogen to come through the delivery hose rapidly while the refill tube

1201 cools down and ensure it is pointed towards a Styrofoam surface or similar receptacle
1202 designed for cryogen storage.

1203

1204 34) Power the cryo-stage by connecting the power cable (cable 1)

1205 35) Place the external dewar such that the liquid nitrogen outlet is in position above the filing
1206 aperture of the cryo-stage

1207 36) Connect it to the cryo-stage via the attached cable (cable 4). Filling of the stage cryogen
1208 store will commence automatically.

1209

1210 **CRITICAL STEP** Check the Linkam stage and ensure that all cables are properly connected;
1211 as seen in **Figure 7** from left to right check: power cable (1), cable for heated stage lid (2),
1212 cable for attaching the digital remote control (3), cable for external auto-refill dewar (4), cable
1213 to control the stage via software and for firmware updates (5).

1214 **CRITICAL STEP** Remain by the cryo-stage while the stage cryogen store is being filled and
1215 ensure it doesn't overflow. Filling can be interrupted by opening the external dewar lid, thereby
1216 eliminating the driving overpressure.

1217 **CRITICAL STEP** Should an external storage dewar not be available, the stage cryogen store
1218 can be filled manually but attention should be paid to constant refills so that it does not empty
1219 during operation.

1220

1221 37) Once the internal liquid nitrogen dewar fills for the first time and allowed to settle, the
1222 sample chamber filling option will appear on position 3 of the screen settings display of the
1223 cryo-stage. Press the chamber filling button to allow the transfer of liquid nitrogen from the
1224 internal dewar into the sample chamber. The refilling process will repeat automatically from
1225 this point onwards.

1226

1227 **CRITICAL STEP** If the external storage dewar is running low on liquid nitrogen, an alarm will
1228 sound accompanied by the chamber's LED lights flashing. Action should be taken immediately
1229 to refill the dewar.

1230

1231 38) Transfer the sample containing storage grid box (from Step 30) in the sample chamber of
1232 the cryo-stage.

1233

1234 **CRITICAL STEP** ~~Extra attention is needed when transferring the cassette to the sample~~
1235 ~~imaging bridge to ensure it remains in or proximal to the cryogen at all times.~~

1236 **CRITICAL STEP** Forceps and other handling equipment that direct touch sample grids or
1237 operate in their immediate vicinity should be cooled in liquid nitrogen before use to ensure
1238 samples suffer no devitrification during any of these processes.

1239 39) Load the grid in the standard sample cassette with a pair of pre-cooled forceps.

1240

1241 TROUBLESHOOTING

1242

1243 **CRITICAL STEP** The sample holders are designed as magnetic sandwiches fastening the grid
1244 between two plates. The user should acquire enough proficiency in their use and operation in
1245 advance of securing and transferring a 'real life' sample.

1246 **CRITICAL STEP** Forceps and other handling equipment that direct touch sample grids or
1247 operate in their immediate vicinity should be cooled in liquid nitrogen before use to ensure
1248 samples suffer no devitrification during any of these processes.

1249

1250 40) Mount the cassette on the sample bridge inside the sample chamber.

1251 **CRITICAL STEP** Extra attention is needed when transferring the cassette to the sample
1252 imaging bridge to ensure it remains in or proximal to the cryogen at all times.

1253

1254 **CRITICAL STEP** In a Linkam cryo-stage, the bridge that receives the sample cassette for
1255 imaging should not be subjected to unnecessary force and cassettes should be placed gently
1256 on the designated areas and only lightly pushed against positional pillar to ensure good
1257 placement.

1258

1259 41) Secure the cryo-stage on the appropriate merchant-supplied cryo-stage holder for the
1260 microscope being careful not to trap any of the connected cables, ensure all stage positioning
1261 aids are observed and pins are aligned with respective casing groves (if present) and then lock
1262 the stage on the microscope.

1263 42) On the control PC, select Link.exe and setup your imaging configuration as follows (**Figure**
1264 **7d-f**): First, at the controller menu tab, press 'connect'. Next, at the camera tab, press 'show',
1265 'show camera'. Finally, at the file menu, select 'open microscope file', 'calibration.lmf'.

1266 43) Move the objective you wish to use (typically 50X or 100X) in the viewing position and
1267 ensure that the objective you are using is selected in the Link objectives tab and drag the
1268 camera view box out of the main package and on to the Desktop.

1269 44) Manually, focus on the grid surface as follows: On the microscope control screen, select
1270 the option 'Turret'. Select the 'On' option for the 'TL (transmitted) illumination' and check that
1271 the 'Off' option is selected for 'RL (reflected) illumination'. Choose an empty position on the
1272 filter tab of the microscope screen and focus by using the stage height wheel while looking
1273 down the ocular. Adjust the level of brightness of light on the sample by turning the brightness
1274 wheel.

1275
1276 **CRITICAL STEP** The above configuration works for brightfield imaging; in order to image
1277 fluorescence channels, you need to turn off the 'TL Illumination' and turn on the 'RL
1278 Illumination', then choose the matching filter by selecting the appropriate position on the
1279 control screen.

1280 **CRITICAL STEP** If the user has no access to semi-automated grid mapping (through Link or a
1281 related software), areas of interest can be recorded manually with notes to elaborate on
1282 particulars and be kept until needed for CLXT imaging.

1283 **CRITICAL STEP** Sample grids need to be mapped (automatically or manually) to allow the
1284 efficient use of imaging time allocated on either cryoSIM or cryoSXT. CLXT Facilities providing
1285 access will expect to be provided with mapped grids and users should know in advance which
1286 specific areas of their sample grids they wish to image when on site.

1287
1288 45) Use the external cryo-stage control for sample navigation. Switching between the eye
1289 piece view and camera view can be done either by manually flipping the redirecting mirror or
1290 by clicking the appropriate shortcut button located at the stage.

1291 46) Assess sample for ice formation and fluorescence distribution (**Figure 7g-p**).

1292 1293 **Cryo sample mapping Timing 30-40 minutes**

1294 **CRITICAL** Once a sample grid has been evaluated, sample mapping can ensue. The
1295 following steps are involved in sample mapping on the same set up following Steps 38-46:

1296 47) Select the icon with the LINK software and select camera view. Ensure you are getting a
1297 focused image.

1298 48) On the Link software, click on the 'X, Y move' tab and select the 'wait between the scans'
1299 option.

1300

1301 **CRITICAL STEP** In order to improve the fluorescence signal, select the option 'Camera' next
1302 to the 'X, Y move' tab on the Link software. A new menu will pop-up with options for changing
1303 the camera settings (exposure, shutter, gamma, gain and fps). Adjust accordingly to optimise
1304 recorded signal.

1305 **CRITICAL STEP** If the sample under examination only has a weakly fluorescent profile it is
1306 advisable to dim ambient lighting to help decrease background on the captured images.

1307

1308 49) Press 'start scan' to start the grid mapping and select a directory.

1309 50) Repeat Steps 47-49 in order to attain a brightfield scan and as many fluorescence scans
1310 as needed (a composite 2D grid mosaic and all individual views at full resolution will be stored
1311 automatically in the selected directory).

1312 51) Once sample mapping has been completed, carefully remove the cryo-stage from the
1313 microscope and place the samples back into the storage dewar.

1314 52) Detach the autofill dewar from the cryo-stage by unplugging the auto-filler cable. Let the
1315 stage gradually warm up until the bake-out option appears in position 2 of the screen settings
1316 display of the cryo-stage.

1317 53) Press and hold the bake-out option for the stage to enter bake-out mode (bake-out will
1318 complete automatically at which point an alarm will sound); unplug the power cable and store.

1319

1320 (Optional)

1321

1322 **Data processing and analysis**

1323 54) Composite mosaic files can be uploaded in any image display software (such as
1324 Photoshop, Powerpoint, ImageJ or similar) that allows the user to mark sites of interest. All
1325 such sites should be clearly labelled to allow selection of areas of interest for subsequent
1326 CLXT data collection.

1327

1328 **Timing**

1329 The approximate timing presented here is for one sample/grid with multiple ROIs:

1330

1331 Step 1, preparation of grids: 15 minutes-16 hours

1332 Step 2, seeding or deposition of cells: 10 minutes-48 hours

1333 Steps 3-9, fluorescent labelling: 20-30 minutes

1334 Step 10, fiducial preparation: 20 minutes – 16 hours

1335 Steps 11-31, fiducialisation and plunge freezing: 5-10 minutes

1336 Steps 32-46, sample evaluation: 10-30 minutes

1337 Steps 47-54, sample mapping: 30-40 minutes

1338

Troubleshooting

Troubleshooting advice can be found in **Table 1**.

Anticipated results

The protocol presented here will allow the researcher to critically evaluate the requirements of the project at hand and apply the resulting fiducialisation regime in a straightforward and reproducible fashion. **Supplementary Table 1** and **Supplementary Table 2** summarise the performance characteristics of the fiducial markers tested and have informed the development of **Figure 3** which acts as the proposed guide.

When planning an experiment, it is important to choose an appropriate fiducialisation strategy and this will depend on the particularities of each investigation. Factors that should be considered include cell type, project requirements, available fluorescent signal, data reconstruction potential and correlative markers required. An intimate knowledge of the expected morphology of the subject matter (cell flatness, organelle distribution, interactions expected within and across populations, quiescent or active state, chemical treatment or effects of pathogens) is a necessary pre-requisite before embarking on a CLXT experiment. Knowing what to expect at a top level (gross cell physiology) allows the taking of informed decisions on which organelles can potentially work as fiducials. This, coupled with the knowledge of additional fluorescence of either endogenously produced or administered project-specific fluorophores in turn, narrows the fluorescence channels that are available for registration purposes. Once the organelles and channels available are confirmed other parameters such as availability of fiducials, ease of use and dispersal will come into play. For example, reagents are only useful if they can be sourced in a reliable and timely fashion and batch variability is kept to a minimum. If a reagent has a propensity towards clumping, then the situation will be exaggerated in thicker, round cells. This will invariably give rise to nanoparticle-free areas over their thickest areas (usually nuclei and perinuclear regions) as the capillary tension of blotting pulls all added material to the substrate surface. To consolidate our extensive experience with the multiple fiducial families currently available, we have devised a decision matrix (**Figure 3**) that makes the strategic design of a fiducialisation regime possible. Given that information, the researcher needs to evaluate the suitability of a fiducialisation strategy with respect to the subject matter. Sample sparsity, cell thickness and surface attachment properties should dictate the choice of fiducial marker or a combination of markers to ensure successful data correlation *in silico*. The summary of features presented in **Figure 3** implicitly highlights two key requirements for successful registration of imaging data; the chosen fiducials need to fit both the imaging method at hand

and the requirements imposed by the biological features that are being examined. For example, use of carbon ‘light’ high-accuracy markers such as TetraSpeck nanoparticles would be suited for the inspection of small, well-dispersed samples (bacterial and viruses) or thin areas in larger cells (cytoplasm edge or similar), provided they are distributed evenly in the ROI. However, in thicker areas of cells, well-defined ubiquitous organelles such as mitochondria could provide the bulk of the necessary positioning information. Moreover, as the distribution of nanoparticle markers is by and large confined to the surface of larger cells and tissue sections, organelle markers become extremely relevant in providing axial information for data alignment.

To evaluate the performance of different fiducials here, we calculated 2D and 3D correlation accuracy of registration of CLXT data using each candidate (**Supplementary Figures 2-5**). It has been shown that, the more abundant and evenly dispersed fiducial markers are in an ROI in a given data set, the more points are available for 2D and 3D correlation and the smaller the target registration error⁷⁵. Therefore, wherever possible, the highest number of points were selected for correlation (**Figure 8**). 3D correlation accuracy in specific can be derived by computing the whole predicted error map and can be depicted as either a range of TRE values (in nm) or as a heat map as seen in **Figure 2**. It is important to note that, even dispersal of fiducial markers across the sample is essential in obtaining high accuracy of correlation. For example, using a highly localised population of lipid droplets as correlative markers in an ROI (**Figure 4a-b**) can result in areas of accurate correlation close to the markers with the predicted error increasing further afield (**Figure 4c-d**). Note that in the case of 2D correlation, the TRE represents a distance in the XY plane; in the case of 3D correlation, the TRE number represents the radius of a sphere.

As an overall example of the data we can generate in CLXT and the importance of appropriate registration marker use, we focused on the application of TetraSpeck microspheres which can be easily sourced as 100 or 200 nm fiducials. According to **Figure 3** they perform well in some areas while less so in others. The core (70 nm and 120 nm respectively) is made from a carbon-based polymer and their shell contains blue, green, orange and far-red fluorescent chemicals. They exhibit weak X-ray absorption in soft X-ray tilt series projections although they can be clearly resolved in 3D reconstructed data. TetraSpeck microspheres of 100 nm diameter can be resolved in tomographic reconstructions when resting on the supporting grid (**Figure 9 a-e**) but the high background commonly noted in areas occupied by cells makes it difficult to locate them over cell material. Therefore, in order to easily align cryoSXT projections prior to reconstruction, highly absorbing fiducials, such as gold nanoparticles should ideally be used in conjunction. However, using fluorescent microspheres in a CLXT experiment can be an advantage, especially when more than one fluorescent channel is used and when accurate alignment of

all laser channels used in all directions is required. However, when chromatic shift is mapped in advance to the experiment, internal registration using TetraSpecks is no longer needed¹¹¹. It is important to note that, as these beads are emitting signals in four channels, they are also competing against other tagged structures of interest in terms of fluorescence signal as well as autofluorescence inherent in cells. Moreover, they are normally not visible under brightfield mode. Given these shortcomings, other biological structures such as mitochondria need to be used to bring about high fidelity 3D correlation (**Figure 9f-h**). For CLXT correlation (**Figure 9i-k**), three points in the support film were used as landmarks initially for rough 2D alignment of CLXT data. The 2D TREs were 538 ± 145 , 135 ± 50 , 81 ± 7 , 63 ± 3 , 54 ± 2 and 45 ± 2 nm when 3, 5, 10, 15, 20 and 30 points were used for registration respectively (**Figure 8a**). For 3D correlation, five registered points in mitochondria structures were used for initial rough alignment. The final 3D correlation accuracy included TetraSpeck localization and gave rise to TRE of 230 ± 50 nm when ten points were used (**Figure 8b**).

Given our findings it is clear that not one single fiducial type can fit all experiments and systems. When deciding on fiducial markers for data correlation or registration in a CLXT experiment, it is recommended that fiducials are chosen (a) taking into account sample characteristics and imaging requirements and (b) with the expectation of using a combination where the strength of one marker makes up for the weakness of the other. We expect our decision aid (**Figure 3**) to offer a quick view that portrays the 'highs' and 'lows' of each possible fiducial marker and their complementarity and enable prospective users to design the most appropriate combinations for their particular research subject.

References

1. Peddie, C. J. & Schieber, N. L. The Importance of Sample Processing for Correlative Imaging (or, Rubbish In, Rubbish Out). in *Correlative Imaging* 37–66 (John Wiley & Sons, Ltd, 2019). doi:10.1002/9781119086420.ch3.
2. Sochacki, K. A., Shtengel, G., van Engelenburg, S. B., Hess, H. F. & Taraska, J. W. Correlative super-resolution fluorescence and metal-replica transmission electron microscopy. *Nature Methods* **11**, 305–308 (2014).
3. Löschberger, A., Franke, C., Krohne, G., Linde, S. van de & Sauer, M. Correlative super-resolution fluorescence and electron microscopy of the nuclear pore complex with molecular resolution. *J Cell Sci* **127**, 4351–4355 (2014).
4. Müller-Reichert, T., Srayko, M., Hyman, A., O'Toole, E. T. & McDonald, K. Correlative light and electron microscopy of early *Caenorhabditis elegans* embryos in mitosis. *Methods Cell Biol.* **79**, 101–119 (2007).
5. Watari, N. & Herman, L. Correlative light and electron microscopy of bat islets of Langerhans in hibernating and nonhibernating states. *Am. Zool.* **5**, 678 (1965).
6. Timmermans, F. J. & Otto, C. Contributed review: Review of integrated correlative light and electron microscopy. *Rev Sci Instrum* **86**, 011501 (2015).
7. Betzig, E. *et al.* Imaging Intracellular Fluorescent Proteins at Nanometer Resolution. *Science* **313**, 1642–1645 (2006).
8. Jahn, K. A. *et al.* Correlative microscopy: providing new understanding in the biomedical and plant sciences. *Micron* **43**, 565–582 (2012).
9. Guérin, C. J., Liv, N. & Klumperman, J. It's a Small, Small World. in *Correlative Imaging* 1–21 (John Wiley & Sons, Ltd, 2019). doi:10.1002/9781119086420.ch1.
10. Dubochet, J., McDowell, A. W., Menge, B., Schmid, E. N. & Lickfeld, K. G. Electron microscopy of frozen-hydrated bacteria. *J Bacteriol* **155**, 381–390 (1983).

- 1466 11. Sartori, A. *et al.* Correlative microscopy: Bridging the gap between fluorescence light microscopy
1467 and cryo-electron tomography. *Journal of Structural Biology* **160**, 135–145 (2007).
- 1468 12. Schwartz, C. L., Sarbash, V. I., Ataullakhanov, F. I., McIntosh, J. R. & Nicastro, D. Cryo-
1469 fluorescence microscopy facilitates correlations between light and cryo-electron microscopy and
1470 reduces the rate of photobleaching. *J Microsc* **227**, 98–109 (2007).
- 1471 13. Bharat, T. A. M. & Kukulski, W. Cryo-Correlative Light and Electron Microscopy. in *Correlative*
1472 *Imaging* 137–153 (John Wiley & Sons, Ltd, 2019). doi:10.1002/9781119086420.ch8.
- 1473 14. Hampton, C. M. *et al.* Correlated fluorescence microscopy and cryo-electron tomography of
1474 virus-infected or transfected mammalian cells. *Nat Protoc* **12**, 150–167 (2017).
- 1475 15. Henderson, R. *et al.* Model for the structure of bacteriorhodopsin based on high-resolution
1476 electron cryo-microscopy. *Journal of Molecular Biology* **213**, 899–929 (1990).
- 1477 16. Hoffman, D. P. *et al.* Correlative three-dimensional super-resolution and block-face electron
1478 microscopy of whole vitreously frozen cells. *Science* **367**, (2020).
- 1479 17. Lučić, V., Rigort, A. & Baumeister, W. Cryo-electron tomography: The challenge of doing
1480 structural biology in situ. *J Cell Biol* **202**, 407–419 (2013).
- 1481 18. Beck, M. & Baumeister, W. Cryo-Electron Tomography: Can it Reveal the Molecular Sociology of
1482 Cells in Atomic Detail? *Trends Cell Biol.* **26**, 825–837 (2016).
- 1483 19. Schneider, G. Cryo X-ray microscopy with high spatial resolution in amplitude and phase
1484 contrast. *Ultramicroscopy* **75**, 85–104 (1998).
- 1485 20. Schneider, G. *et al.* Three-dimensional cellular ultrastructure resolved by X-ray microscopy. *Nat.*
1486 *Methods* **7**, 985–987 (2010).
- 1487 21. Groen, J., Conesa, J. J., Valcárcel, R. & Pereiro, E. The cellular landscape by cryo soft X-ray
1488 tomography. *Biophys Rev* **11**, 611–619 (2019).
- 1489 22. Kounatidis, I. *et al.* 3D Correlative Cryo-Structured Illumination Fluorescence and Soft X-ray
1490 Microscopy Elucidates Reovirus Intracellular Release Pathway. *Cell* **182**, 1–16 (2020).
- 1491 23. Le Gros, M. A. *et al.* Biological soft X-ray tomography on beamline 2.1 at the Advanced Light
1492 Source. *J Synchrotron Radiat* **21**, 1370–1377 (2014).

- 1493 24. Sorrentino, A. *et al.* MISTRAL: a transmission soft X-ray microscopy beamline for cryo nano-
1494 tomography of biological samples and magnetic domains imaging. *Journal of Synchrotron*
1495 *Radiation* **22**, 1112–1117 (2015).
- 1496 25. Mahamid, J. *et al.* Visualizing the molecular sociology at the HeLa cell nuclear periphery. *Science*
1497 **351**, 969–972 (2016).
- 1498 26. Phillips, M. *et al.* CryoSIM: super resolution 3D structured illumination cryogenic fluorescence
1499 microscopy for correlated ultra-structural imaging. *Optica* **7**, 802–812 (2020).
- 1500 27. Kaufmann, R., Hagen, C. & Grünewald, K. Super-resolution fluorescence microscopy of cryo-
1501 immobilized samples. in *European Microscopy Congress 2016: Proceedings* 1017–1017
1502 (American Cancer Society, 2016). doi:10.1002/9783527808465.EMC2016.6928.
- 1503 28. Kaufmann, R. *et al.* Super-Resolution Microscopy Using Standard Fluorescent Proteins in Intact
1504 Cells under Cryo-Conditions. *Nano Lett.* **14**, 4171–4175 (2014).
- 1505 29. Kaufmann, R., Hagen, C. & Grünewald, K. Fluorescence cryo-microscopy: current challenges and
1506 prospects. *Current Opinion in Chemical Biology* **20**, 86–91 (2014).
- 1507 30. Duke, E. M. H. *et al.* Imaging endosomes and autophagosomes in whole mammalian cells using
1508 correlative cryo-fluorescence and cryo-soft X-ray microscopy (cryo-CLXM). *Ultramicroscopy* **143**,
1509 77–87 (2014).
- 1510 31. Fokkema, J. *et al.* Fluorescently Labelled Silica Coated Gold Nanoparticles as Fiducial Markers for
1511 Correlative Light and Electron Microscopy. *Scientific Reports* **8**, 1–10 (2018).
- 1512 32. Geissinger, H. D. A precise stage arrangement for correlative microscopy for specimens mounted
1513 on glass slides, stubs or EM grids. *Journal of Microscopy* **100**, 113–117 (1974).
- 1514 33. Su, Y. *et al.* Multi-dimensional correlative imaging of subcellular events: combining the strengths
1515 of light and electron microscopy. *Biophys Rev* **2**, 121–135 (2010).
- 1516 34. Fluorophores. in *Principles of Fluorescence Spectroscopy* (ed. Lakowicz, J. R.) 63–95 (Springer US,
1517 2006). doi:10.1007/978-0-387-46312-4_3.
- 1518 35. Lavis, L. D. & Raines, R. T. Bright Ideas for Chemical Biology. *ACS Chem Biol* **3**, 142–155 (2008).

- 1519 36. Anderson, K., Nilsson, T. & Fernandez-Rodriguez, J. Challenges for CLEM from a Light Microscopy
1520 Perspective. in *Correlative Imaging* 23–35 (John Wiley & Sons, Ltd, 2019).
1521 doi:10.1002/9781119086420.ch2.
- 1522 37. Paul-Gilloteaux, P. & Schorb, M. Correlating Data from Imaging Modalities. in *Correlative*
1523 *Imaging* 191–210 (John Wiley & Sons, Ltd, 2019). doi:10.1002/9781119086420.ch11.
- 1524 38. Pereiro, E., Chichón, F. J. & Carrascosa, J. L. Correlative Cryo Soft X-ray Imaging. in *Correlative*
1525 *Imaging* 155–169 (John Wiley & Sons, Ltd, 2019). doi:10.1002/9781119086420.ch9.
- 1526 39. Rizk, A. *et al.* Segmentation and quantification of subcellular structures in fluorescence
1527 microscopy images using Squassh. *Nat Protoc* **9**, 586–596 (2014).
- 1528 40. Pereiro, E., Nicolás, J., Ferrer, S. & Howells, M. R. A soft X-ray beamline for transmission X-ray
1529 microscopy at ALBA. *J Synchrotron Rad* **16**, 505–512 (2009).
- 1530 41. Harkiolaki, M. *et al.* Cryo-soft X-ray tomography: using soft X-rays to explore the ultrastructure
1531 of whole cells. *Emerging Topics in Life Sciences* **2**, 81–92 (2018).
- 1532 42. Gustafsson, M. G. L. *et al.* Three-dimensional resolution doubling in wide-field fluorescence
1533 microscopy by structured illumination. *Biophys J* **94**, 4957–4970 (2008).
- 1534 43. Carrascosa, J. L. *et al.* Cryo-X-ray tomography of vaccinia virus membranes and inner
1535 compartments. *Journal of Structural Biology* **168**, 234–239 (2009).
- 1536 44. Pérez-Berná, A. J. *et al.* Structural Changes In Cells Imaged by Soft X-ray Cryo-Tomography
1537 During Hepatitis C Virus Infection. *ACS Nano* **10**, 6597–6611 (2016).
- 1538 45. Spink, M. C. *et al.* Correlation of Cryo Soft X-ray Tomography with Cryo Fluorescence Microscopy
1539 to Characterise Cellular Organelles at Beamline B24, Diamond Light Source. *Microscopy and*
1540 *Microanalysis* **24**, 374–375 (2018).
- 1541 46. Bohren, C. F. & Huffman, D. R. *Absorption and Scattering of Light by Small Particles*. (John Wiley
1542 & Sons, 2008).
- 1543 47. Kerker, M. *The Scattering of Light and Other Electromagnetic Radiation: Physical Chemistry: A*
1544 *Series of Monographs*. (Academic Press, 2013).

- 1545 48. Kreibig, U. & Vollmer, M. *Optical Properties of Metal Clusters*. (Springer Science & Business
1546 Media, 2013).
- 1547 49. Papavassiliou, G. C. Optical properties of small inorganic and organic metal particles. *Progress in*
1548 *Solid State Chemistry* **12**, 185–271 (1979).
- 1549 50. Weiner, A. *et al.* Vitrification of thick samples for soft X-ray cryo-tomography by high pressure
1550 freezing. *J. Struct. Biol.* **181**, 77–81 (2013).
- 1551 51. Gal, A. *et al.* Native-state imaging of calcifying and noncalcifying microalgae reveals similarities
1552 in their calcium storage organelles. *PNAS* **115**, 11000–11005 (2018).
- 1553 52. Conesa, J. J. *et al.* Unambiguous Intracellular Localization and Quantification of a Potent Iridium
1554 Anticancer Compound by Correlative 3D Cryo X-Ray Imaging. *Angewandte Chemie (International*
1555 *Ed. in English)* **59**, 1270–1278 (2020).
- 1556 53. Ando, T. *et al.* The 2018 correlative microscopy techniques roadmap. *J Phys D Appl Phys* **51**,
1557 443001 (2018).
- 1558 54. Arnold, J. *et al.* Site-Specific Cryo-focused Ion Beam Sample Preparation Guided by 3D
1559 Correlative Microscopy. *Biophys J* **110**, 860–869 (2016).
- 1560 55. Kukulski, W. *et al.* Correlated fluorescence and 3D electron microscopy with high sensitivity and
1561 spatial precision. *J Cell Biol* **192**, 111–119 (2011).
- 1562 56. de Boer, P., Hoogenboom, J. P. & Giepmans, B. N. G. Correlated light and electron microscopy:
1563 ultrastructure lights up! *Nature Methods* **12**, 503–513 (2015).
- 1564 57. Varsano, N. *et al.* Development of Correlative Cryo-soft X-ray Tomography and Stochastic
1565 Reconstruction Microscopy. A Study of Cholesterol Crystal Early Formation in Cells. *Journal of*
1566 *the American Chemical Society* **138**, 14931–14940 (2016).
- 1567 58. Hagen, C. *et al.* Multimodal nanoparticles as alignment and correlation markers in
1568 fluorescence/soft X-ray cryo-microscopy/tomography of nucleoplasmic reticulum and apoptosis
1569 in mammalian cells. *Ultramicroscopy* **146**, 46–54 (2014).

- 1570 59. Elgass, K. D., Smith, E. A., LeGros, M. A., Larabell, C. A. & Ryan, M. T. Analysis of ER-mitochondria
1571 contacts using correlative fluorescence microscopy and soft X-ray tomography of mammalian
1572 cells. *Journal of Cell Science* **128**, 2795–2804 (2015).
- 1573 60. McDermott, G., Le Gros, M. A., Knoechel, C. G., Uchida, M. & Larabell, C. A. Soft X-ray
1574 tomography and cryogenic light microscopy: the cool combination in cellular imaging. *Trends in*
1575 *Cell Biology* **19**, 587–595 (2009).
- 1576 61. Kapishnikov, S. *et al.* Unraveling heme detoxification in the malaria parasite by in situ correlative
1577 X-ray fluorescence microscopy and soft X-ray tomography. *Scientific Reports* **7**, 7610 (2017).
- 1578 62. Smith, E. A. *et al.* Quantitatively imaging chromosomes by correlated cryo-fluorescence and soft
1579 x-ray tomographies. *Biophysical Journal* **107**, 1988–1996 (2014).
- 1580 63. Hest, J. J. H. a. V. *et al.* Towards robust and versatile single nanoparticle fiducial markers for
1581 correlative light and electron microscopy. *Journal of Microscopy* **274**, 13–22 (2019).
- 1582 64. Aslan, K., Wu, M., Lakowicz, J. R. & Geddes, C. D. Fluorescent core-shell Ag@SiO₂
1583 nanocomposites for metal-enhanced fluorescence and single nanoparticle sensing platforms. *J.*
1584 *Am. Chem. Soc.* **129**, 1524–1525 (2007).
- 1585 65. Aslan, K. & Geddes, C. D. Metal-Enhanced Fluorescence: Progress Towards a Unified Plasmon-
1586 Fluorophore Description. in *Metal-Enhanced Fluorescence* 1–23 (John Wiley & Sons, Ltd, 2010).
1587 doi:10.1002/9780470642795.ch1.
- 1588 66. Lee, D., Lee, J., Song, J., Jen, M. & Pang, Y. Homogeneous silver colloidal substrates optimal for
1589 metal-enhanced fluorescence. *Phys. Chem. Chem. Phys.* **21**, 11599–11607 (2019).
- 1590 67. Hodgson, L., Verkade, P. & Yamauchi, Y. Correlative Light and Electron Microscopy of Influenza
1591 Virus Entry and Budding. *Influenza Virus* 237–260 (2018) doi:10.1007/978-1-4939-8678-1_12.
- 1592 68. McGorty, R., Kamiyama, D. & Huang, B. Active Microscope Stabilization in Three Dimensions
1593 Using Image Correlation. *Opt Nanoscopy* **2**, (2013).
- 1594 69. Metskas, L. A. & Briggs, J. A. G. Fluorescence-Based Detection of Fusion State on a Cryo-EM Grid
1595 using Correlated Cryo-Fluorescence and Cryo-Electron Microscopy. *bioRxiv* 388579 (2018)
1596 doi:10.1101/388579.

- 1597 70. Walling, M. A., Novak, J. A. & Shepard, J. R. E. Quantum Dots for Live Cell and In Vivo Imaging.
1598 *Int J Mol Sci* **10**, 441–491 (2009).
- 1599 71. Wegner, K. D. & Hildebrandt, N. Quantum dots: bright and versatile in vitro and in vivo
1600 fluorescence imaging biosensors. *Chem. Soc. Rev.* **44**, 4792–4834 (2015).
- 1601 72. Hemelaar, S. R. *et al.* Nanodiamonds as multi-purpose labels for microscopy. *Scientific Reports* **7**,
1602 1–9 (2017).
- 1603 73. Schade, A. E. *et al.* Dasatinib, a small-molecule protein tyrosine kinase inhibitor, inhibits T-cell
1604 activation and proliferation. *Blood* **111**, 1366–1377 (2008).
- 1605 74. Trickett, A. & Kwan, Y. L. T cell stimulation and expansion using anti-CD3/CD28 beads. *Journal of*
1606 *Immunological Methods* **275**, 251–255 (2003).
- 1607 75. Paul-Gilloteaux, P. *et al.* eC-CLEM: flexible multidimensional registration software for correlative
1608 microscopies. *Nature Methods* **14**, 102–103 (2017).
- 1609 76. Bogovic, J. A., Hanslovsky, P., Wong, A. & Saalfeld, S. Robust registration of calcium images by
1610 learned contrast synthesis. in *2016 IEEE 13th International Symposium on Biomedical Imaging*
1611 *(ISBI)* 1123–1126 (2016). doi:10.1109/ISBI.2016.7493463.
- 1612 77. de Chaumont, F. *et al.* Icy: an open bioimage informatics platform for extended reproducible
1613 research. *Nature Methods* **9**, 690–696 (2012).
- 1614 78. Miles, B. T. *et al.* Direct Evidence of Lack of Colocalisation of Fluorescently Labelled Gold Labels
1615 Used in Correlative Light Electron Microscopy. *Sci Rep* **7**, (2017).
- 1616 79. Oorschot, V., de Wit, H., Annaert, W. G. & Klumperman, J. A novel flat-embedding method to
1617 prepare ultrathin cryosections from cultured cells in their in situ orientation. *J. Histochem.*
1618 *Cytochem.* **50**, 1067–1080 (2002).
- 1619 80. Tuijtel, M. W., Koster, A. J., Jakobs, S., Faas, F. G. A. & Sharp, T. H. Correlative cryo super-
1620 resolution light and electron microscopy on mammalian cells using fluorescent proteins.
1621 *Scientific Reports* **9**, 1369 (2019).
- 1622 81. Schellenberger, P. *et al.* High-precision correlative fluorescence and electron cryo microscopy
1623 using two independent alignment markers. *Ultramicroscopy* **143**, 41–51 (2014).

- 1624 82. Pezzi, H. M., Niles, D. J., Schehr, J. L., Beebe, D. J. & Lang, J. M. Integration of Magnetic Bead-
1625 Based Cell Selection into Complex Isolations. *ACS omega* **3**, 3908–3917 (2018).
- 1626 83. Uludag, H., Ubeda, A. & Ansari, A. At the Intersection of Biomaterials and Gene Therapy:
1627 Progress in Non-viral Delivery of Nucleic Acids. *Frontiers in Bioengineering and Biotechnology* **7**,
1628 131 (2019).
- 1629 84. Booth, D. G., Beckett, A. J., Prior, I. A. & Meijer, D. SuperCLEM: an accessible correlative light and
1630 electron microscopy approach for investigation of neurons and glia in vitro. *Biology Open* **8**,
1631 (2019).
- 1632 85. Tuijtel, M. W., Koster, A. J., Jakobs, S., Faas, F. G. A. & Sharp, T. H. Correlative cryo super-
1633 resolution light and electron microscopy on mammalian cells using fluorescent proteins.
1634 *Scientific Reports* **9**, 1–11 (2019).
- 1635 86. Telling, N. D. *et al.* Iron Biochemistry is Correlated with Amyloid Plaque Morphology in an
1636 Established Mouse Model of Alzheimer’s Disease. *Cell Chemical Biology* **24**, 1205-1215.e3
1637 (2017).
- 1638 87. Jamme, F. *et al.* Synchrotron multimodal imaging in a whole cell reveals lipid droplet core
1639 organization. *J Synchrotron Rad* **27**, 772–778 (2020).
- 1640 88. Ahn, S., Jung, S. Y. & Lee, S. J. Gold Nanoparticle Contrast Agents in Advanced X-ray Imaging
1641 Technologies. *Molecules* **18**, 5858–5890 (2013).
- 1642 89. Niclis, J. C. *et al.* Three-dimensional imaging of human stem cells using soft X-ray tomography.
1643 *Journal of The Royal Society Interface* **12**, 20150252 (2015).
- 1644 90. Conesa, J. J. *et al.* Intracellular nanoparticles mass quantification by near-edge absorption soft X-
1645 ray nanotomography. *Scientific Reports* **6**, 22354 (2016).
- 1646 91. Matsuda, A., Schermelleh, L., Hirano, Y., Haraguchi, T. & Hiraoka, Y. Accurate and fiducial-
1647 marker-free correction for three-dimensional chromatic shift in biological fluorescence
1648 microscopy. *Scientific Reports* **8**, 7583 (2018).
- 1649 92. Schindelin, J. *et al.* Fiji: an open-source platform for biological-image analysis. *Nature Methods* **9**,
1650 676–682 (2012).

1651 93. Ball, G. *et al.* SIMcheck: a Toolbox for Successful Super-resolution Structured Illumination
1652 Microscopy. *Scientific Reports* **5**, 15915 (2015).

1653 94. Kremer, J. R., Mastronarde, D. N. & McIntosh, J. R. Computer visualization of three-dimensional
1654 image data using IMOD. *J. Struct. Biol.* **116**, 71–76 (1996).

1655 95. Luengo, I. *et al.* SuRVoS: Super-Region Volume Segmentation workbench. *Journal of Structural*
1656 *Biology* **198**, 43–53 (2017).

1657 96. Goddard, T. D. *et al.* UCSF ChimeraX: Meeting modern challenges in visualization and analysis.
1658 *Protein Sci* **27**, 14–25 (2018).

1659 97. Bouterfa, H. *et al.* Expression of different extracellular matrix components in human brain tumor
1660 and melanoma cells in respect to variant culture conditions. *Journal of Neuro-Oncology* **44**, 23–
1661 33 (1999).

1662 98. Vaz, F. *et al.* Accessibility to Peptidoglycan Is Important for the Recognition of Gram-Positive
1663 Bacteria in *Drosophila*. *Cell Reports* **27**, 2480–2492.e6 (2019).

1664 99. Vizcardo, R. *et al.* Regeneration of human tumor antigen-specific T cells from iPSCs derived from
1665 mature CD8(+) T cells. *Cell Stem Cell* **12**, 31–36 (2013).

1666 100. Peng, T. *et al.* Determining the distribution of probes between different subcellular locations
1667 through automated unmixing of subcellular patterns. *Proceedings of the National Academy of*
1668 *Sciences of the United States of America* **107**, 2944–2949 (2010).

1669 101. Farmer, B. C., Kluemper, J. & Johnson, L. A. Apolipoprotein E4 Alters Astrocyte Fatty Acid
1670 Metabolism and Lipid Droplet Formation. *Cells* **8**, (2019).

1671 102. Chazotte, B. Labeling lysosomes in live cells with LysoTracker. *Cold Spring Harbor Protocols*
1672 **2011**, pdb.prot5571 (2011).

1673 103. Bianchini, P. *et al.* Live imaging of mammalian retina: rod outer segments are stained by
1674 conventional mitochondrial dyes. *Journal of Biomedical Optics* **13**, 054017 (2008).

1675 104. Awasthi, S., Madhusoodhanan, R. & Wolf, R. Surfactant protein-A and toll-like receptor-4
1676 modulate immune functions of preterm baboon lung dendritic cell precursor cells. *Cellular*
1677 *Immunology* **268**, 87–96 (2011).

105. Drulyte, I. *et al.* Approaches to altering particle distributions in cryo-electron microscopy sample preparation. *Acta Crystallographica. Section D, Structural Biology* **74**, 560–571 (2018).
106. Thompson, R. F., Walker, M., Siebert, C. A., Muench, S. P. & Ranson, N. A. An introduction to sample preparation and imaging by cryo-electron microscopy for structural biology. *Methods (San Diego, Calif.)* **100**, 3–15 (2016).
107. Grassucci, R. A., Taylor, D. J. & Frank, J. Preparation of macromolecular complexes for cryo-electron microscopy. *Nature Protocols* **2**, 3239–3246 (2007).
108. Hiroyasu, A., DeWitt, D. C. & Goodman, A. G. Extraction of Hemocytes from *Drosophila melanogaster* Larvae for Microbial Infection and Analysis. *J Vis Exp* (2018) doi:10.3791/57077.
109. Dobro, M. J., Melanson, L. A., Jensen, G. J. & McDowell, A. W. Chapter Three - Plunge Freezing for Electron Cryomicroscopy. in *Methods in Enzymology* (ed. Jensen, G. J.) vol. 481 63–82 (Academic Press, 2010).
110. Noble, A. J. *et al.* Routine single particle CryoEM sample and grid characterization by tomography. *eLife* **7**, (2018).
111. Schellenberger, P. *et al.* High-precision correlative fluorescence and electron cryo microscopy using two independent alignment markers. *Ultramicroscopy* **143**, 41–51 (2014).

1696 **Table 1: Troubleshooting common issues and recommended action.**

Step(s)	Problem	Possible reason	Solution
1	Torn carbon film on grid.	Rough handling of grids with the forceps.	Gentle handling of grids with forceps.
		Twisted forceps tips during transfer.	Visually inspect all forceps before use.
		Forced loading while grid is not in optimal orientation.	Load samples carefully keeping your eyes on the grid at all times.
2	Too little or too many cells per square in a grid.	Low or high cell seeding density.	Seed at the appropriate density.
			Allow the cells to grow for longer if density is low.
			Grow the cells for a shorter time frame if density is high.
7	Oversaturation of fluorescence signal and lots of pixel counts in cryoSIM.	High concentration of fluorescent dye/tracker was used.	Reduce (optimise) the concentration and timing of fluorescent tracker used.
7	Fluorescence signal is too low.	Low concentration of fluorescent dye/tracker was used.	Increase (optimise) the concentration and timing of fluorescent tracker used.
10	Fiducials aggregate in the vitrified sample.	Stock solution of fiducials have precipitated as they have been stationary.	Thoroughly vortex the stock solution before taking out from it for dilution.
		Diluted fiducials were not well dispersed prior to fiducialisation.	Vortex the fiducial solutions properly. Sonication can be used for further dispersal.
		If DMEM with FBS was used for dilution, serum could lead to aggregation of nanoparticles.	Consider using another buffer for dilution (e.g ddH ₂ O or TBS).
		Current batch of fiducials is over its expiration date.	Use a new batch.
10	Fiducial stock has fewer nanoparticles.	The stock was not shaken enough before taking solution out of it	Shake the stock solution for a longer time before taking out any volume for

		for dilution.	use.
25	Thick ice on the sample.	Inadequate blotting.	Increase blotting time to acceptable levels.
		Cells may be too confluent.	Reduce the seeding density of cells or reduce cell culture time.
30, 39	Large deposit of solid ice crystals on the grid.	Atmospheric ice contamination.	Increase the grid transfer speed.
			Perform vitrification and grid transfers in a humidity-controlled environment (<20% relative humidity).

1697

1698

Figure Legends

Figure 1. Flow chart showing the correlative cryo-light/fluorescence and soft X-ray microscopy fiducialisation workflow described in this study.

All steps in this fiducialisation scheme are presented with related timeframes for a single sample-containing grid with multiple imaging domains. Illustrative images in panels (bottom) show the resulting benefit in sequential imaging using representative data from a region of interest within the cytoplasm of an NIH-3T3 cell. In this ROI, mitochondria were stained with MitoTracker dye (red) and imaged with cryoSIM and then cryoSXT. Data were correlated with eC-CLEM using image registration markers added according to the protocol presented here.

Figure 2. Illustration of 2D (cryoSIM only and cryoSIM on X-ray mosaic) and 3D (cryoSXT only and cryoSIM with cryoSXT) correlation using commercially available fiducial markers and organelle trackers.

Each row shows from left to right: the type of fiducial under evaluation; 2D cryoSIM image (2D cryoSIM refers to a single plane from a 3D cryoSIM reconstructed image stack); 2D correlation of cryoSIM data with X-ray mosaic of the respective area; X-ray tomogram slice of an ROI within the same area; 3D correlation of cryoSIM and cryoSXT in this ROI; associated error map for the 3D correlation (generated in eC-CLEM). 2D and 3D correlation using: **(a)**, fluorescent TetraSpeck microspheres (in green) with NIH-3T3 cells; the mitochondria in these cells were labelled with MitoTracker red as reference; **(b)**, green fluorescent nanodiamonds as fiducials with U2OS cells (mitochondria labelled with MitoTracker red for reference); **(c)**, red fluorescent gold nanoparticles with U2OS cells (mitochondria labelled with MitoTracker green); **(d)**, fluorescently labelled lipid droplets (in green) in U2OS cells (mitochondria labelled with MitoTracker red); **(e)**, fluorescently labelled mitochondria (MitoTracker red) in NIH-3T3 cells; **(f)**, fluorescently labelled lysosomes in *Drosophila* primary post-embryonic plasmatocytes (lysosomes labelled with LysoTracker red). **(g)**, fluorescent magnetic beads (Dynabeads) as fiducials for human primary CD8+ T cells (mitochondria labelled with MitoTracker red). Scale bars according to columns: 2D cryoSIM (10 μm); 2D cryoSIM-cryoSXT (10 μm); 3D cryoSXT (5 μm); 3D cryoSIM-cryoSXT (5 μm). Colour bar in correlation column black to white: **(a)**, 60-170 nm; **(b)** 60-510 nm; **(c)** 60-200 nm; **(d)** 60-410 nm **(e)**, 60-220 nm; **(f)** 60-290 nm; **(g)** 60-540 nm.

Figure 3: Decision making scheme for use of fiducials for CLXT.

Assessment of performance of individual fiducial markers based on parameters that could impact on project feasibility and ease such as availability of raw material and imaging characteristics. The ticks represent acceptable performance specific to each of these fields and should be used as a simple yes/no indicator in deciding on a robust fiducialisation scheme. Users are advised to consider all of these parameters based on their resources and subject matter and include a combination of fiducials in their sample preparation that will allow them to accumulate ticks for all these parameters for efficient correlative imaging. A traffic lights colour scheme has been applied with: dark green for excellent performance (optimal for use), light green for good performance (applicable with some caveats), orange for moderate performance (may not work well) and red for poor performance (does not deliver in this field). Further details on the parameters used can be found in **Supplementary Table 1** and **Supplementary Table 2**. **Supplementary Figures 2-5** show representative data that were used to assess the suitability of each potential fiducial type for CLXT.

Figure 4. Demonstration of correlation of fluorescence and X-ray data in U2OS cells using green lipid droplets as fiducial markers.

(a), Slice of 3D fluorescence image obtained from cryoSIM with a ROI expanded as inset. Lipid droplets (blue arrow) were labelled with green-fluorescent dye, mitochondria (magenta arrow) with red-fluorescent dye and endoplasmic reticulum tracker signal is shown in blue (note that the ER tracker used here interacted with extracellular regions proximal to the cell membrane in a non-specific manner increasing the background in that channel). **(b)**, X-ray mosaic of the same sample and ROI expanded as inset. **(c)**, 2D alignment of X-ray mosaic with cumulative Z projection of the corresponding cryoSIM data and a slice of the 3D correlated volumes at the ROI as an inset. 3D correlation error/heat maps using **(d)**, 5 or **(e)**, 10 lipid droplets as fiducials. Scale bars: **(a)-(c)** 10 μm ; insets **(a)-(c)** 5 μm . Colour bars black to white: **(d)**, 90-520 nm **(e)**, 60-410 nm.

Figure 5. Examples of equipment used for sample support preparation, fiducial dispersal and sample vitrification through plunge freezing.

(a), PELC easiGlow discharge unit for glow discharge of EM grids shown in **(i)**. **(b)**, Glow discharge unit with glass slide placed on the metal sample stand and **(c)**, the same with the glass cover forming the vacuum chamber. **(d)**, Fisherbrand ultrasonic bath sonicator used for dispersing nanoparticles and **(e)**, sonicator bath filled with ddH₂O and ice used for nanoparticle dispersal (nanoparticle suspension in the microcentrifuge tube seen). **(f)**, Leica

GP2 plunge freezer used for sample vitrification (inset shows a sample carrying grid loaded in place). **(i)**, Same as **(g)** in 'lower chamber' position. **(h)**, Ethane gas unit with safety valves and the Leica GP2 sample lid for ethane delivery. **(i)** A 3 mm gold grid held with fine-tip inverted forceps. Yellow arrows in panels point to EM grid/sample position.

Figure 6. Optimization of 250 nm gold fiducial dispersion using sonication and dispersal in different media.

Nanoparticles sonicated and dispersed in **(a)**, water **(b)**, TBS buffer **(c)**, DMEM media and **(d)**, DMEM media supplemented with FBS. **(e)**, Nanoparticles dispersed in 10% (wt/vol) BSA. Closeups of selected areas provided as insets for clarity. Our testing indicates that if the nanoparticles need to be added in a cell-friendly (isotonic and neutral) solution, sonication helps even dispersion provided serum is not included. If 10% (wt/vol) BSA is a viable alternative for the experiment, it offers the best dispersal with minimal handling. Scale bars are 50 μm for all main panels **(a)-(e)** and 10 μm for all insets.

Figure 7. Conventional cryo-microscopy setup, mapping software and sample evaluation.

(a), Zeiss AxioImager2 coupled to a Linkam CMS196M LED cryo-stage with external liquid nitrogen dewar and a control PC using the LINK system control and image capture software. **(b)**, Cryo-stage on external stage holder with power (1), heated stage lid (2), digital remote control (3), external auto-refill dewar (4) and software control (5) connections. **(c)**, Microscope control screen with imaging options. **(d)**, Typical brightfield mapped finder grid populated with cells. **(e)**, LINK software submenu. **(f)-(o)**, Maps of representative grids showing optimal and suboptimal samples with zoomed views as insets. **(f)** and **(g)**, Typical mapping of sample on a grid (mammalian HFF cells in this case) viewed in brightfield and fluorescence respectively; this cell distribution provides areas without cells available for blotting, cells are confluent enough to expect minimal flattening and associated damage, minimal contamination from crystalline ice and other particulates and, no cracks on the substrate or the vitrified sample. **(h)**, Grid map with optimal sample coverage (40-70% confluency for adherent cells). **(i)**, Panel shows good blotting with typical meniscus indicating that media have not been completely drained during blotting. **(j)**, An overconfluent sample with complete surface coverage making it unlikely to have been blotted well and unlikely to have vitrified well; cryoSXT data collection will be difficult for such a sample due to limited penetration by X-rays. **(k)**, A low confluency grid which is likely to have flattened cells and possibly cell damage during blotting. **(l)**, Support film damage due to mechanical forces

(likely mishandling during manual transfer). **(m)**, Heavy ice contamination, probably the result of partial thawing during transfer or storage in unfiltered liquid nitrogen. **(n)**, Grid that has not been blotted well (or at all) and as a result a thick layer of vitreous ice has formed leading to cracks formed when the grid is placed in the microscope holders and forced to adopt a flat geometry. **(o)**, Grid showing thick vitreous areas (as evidenced by the extensive network of cracks) and heating damage through handling with tweezers that were not cooled properly. Samples resembling the examples in panels **(k)** to **(o)** should be avoided and are usually not suitable for further CLXT imaging.

Figure 8. Representation of target registration error (TRE) values for different fiducial markers using eC-CLEM.

Graphical representation of TRE for **(a)**, different fiducials when the same number of registration points were used during 2D correlation **(b)**, TRE for different fiducials when the same number of registration points were used during 3D correlation. Data shown as Mean \pm Standard deviation (excluding 3D correlation with Dynabeads) including individual points. $n = 3$ datasets per fiducial marker (excluding 2D correlation with Dynabeads where $n = 2$ from 3-20 points and 3D correlation with Dynabeads where $n = 1$ at 10 points).

Figure 9. Correlation of CLXT data with TetraSpeck microspheres.

(a), Fluorescent signal from the TetraSpecks in the green channel collected at the cryoSIM; the beads are on the surface of the support film. **(b)**, Single slice from the reconstructed cryoSXT volume (the X-ray field of view is marked with a yellow box in panel **(a)**). **(c)**, Correlation of **(a)** and **(b)**. **(d)**, Fiducials (area boxed in red in **(c)**) in the XY plane and **(e)**, in the XZ plane. **(f)**, Single slice of cryoSIM data showing mitochondria (red) and microspheres (green). **(g)**, 2D X-ray mosaic of the area in **(f)**. **(h)**, Correlation of fluorescence **(f)** and X-ray **(g)** data using mitochondrial signal for rough alignment and TetraSpecks as fiducial markers for fine alignment in 3D. **(i)**, 2D X-ray mosaic of the boxed blue area in **(g)** with single slices from five reconstructed 3D cryoSXT tomograms superimposed as insets. **(j)**, Same area showing the observed green fluorescence microsphere signal. **(k)**, 3D correlation of fluorescence data **(j)**, and X-ray tomograms **(i)**. Scale bars are: in **(a)** 5 μm , **(b)** and **(c)** 2 μm , **(d)** and **(e)** 0.5 μm , **(f)** to **(h)** 10 μm , **(i)** and **(k)** 10 μm , **(j)** 5 μm .

Acknowledgements

Our thanks to Perrine Paul-Gilloteaux for her invaluable help with eC-CLEM, previous and current members of the B24 and BL09 teams with special thanks to Matt Spink for instrumentation support and Adam Taylor and Adam Prescott for technical support. Many thanks also to Aled Clayton for suggestions in trying new reagents and Maud Dumoux for help with laboratory techniques, advice and training. We would like to acknowledge the support of Micron in the development, application and maintenance of the B24 super resolution facility. We also thank Dr. Antonio Aires Trapote (CIC BiomaGUNE, San Sebastian, Spain), Dr. Ana V. Villar, Dr. Ana R. Palanca, David Maestro Lavín (IBBTEC, Santander, Spain) and Dr. Javier Conesa (ALBA and CNB-CSIC). This work was carried out with the support of the Diamond Light Source, instrument B24 (proposals MX18737, MX20321, BI22274, BI23046 and BI25162). We acknowledge ALBA for allocated MISTRAL beamtimes 2018093099 and 2019093739. This project has received funding from the European Commission Horizon 2020 iNEXT-Discovery project and the European Union's Horizon 2020 research and innovation program under the Marie Skłodowska-Curie grant agreement No 75439 and Wellcome awards 091911/Z/11/Z, 107457/Z/15/Z. SB is supported by ERC AdG670930.

Author contributions

C.A.O. coordinated and produced the manuscript with the help of I.K., J.G, E.P. & M.H.. C.A.O., I.K, J.G., A.L.C., K.L.N. and S.B provided data, protocols and critical evaluation of results. M.K. and T.M.F. provided support with software and protocol development. I.M.D. supported cryoSIM operations and optimisation. E.P. and M.H. managed beamline resources, supervised experiments and evaluated applicability and user-friendliness.

Competing interests

The authors declare no competing interests.

Data availability

Original imaging data referenced in the manuscript are deposited at the BioImage Archive (<https://www.ebi.ac.uk/biostudies/BiolImages>) and EMPIAR (<https://www.ebi.ac.uk/pdbe/emdb/empiar/>). The accession numbers for the data are

1874 EMPIAR: EMPIAR-10617, EMPIAR-10618, EMPIAR-10619, EMPIAR-10620, EMPIAR-
1875 10621, EMPIAR-10622, EMPIAR-10624, and BioImage Archive: S-BIAD36, S-BIAD37, S-
1876 BIAD38, S-BIAD39, S-BIAD40, S-BIAD41 and S-BSST576.

1877

1878 **Related links**

1879 Key references using this protocol:

1880 Kounatidis, I. *et al. Cell* **182**, 1–16 (2020). <https://doi.org/10.1016/j.cell.2020.05.051>

1881 Phillips, M. *et al. Optica* **7**, 802–812 (2020). <https://doi.org/10.1364/OPTICA.393203>

1882 Harkiolaki, M. *et al. Emerging Topics in Life Sciences* **2**, 81–92 (2018).

1883 <https://doi.org/10.1042/ETLS20170086>

1884

1885 **SUPPLEMENTARY INFORMATION**

1886 **Supplementary Note 1. ...**

1887

Sample Preparation for CLXT

Preparation of sample grids (Step 1)

Time: 15 min - 16 h

Seeding and
culture of cells
(Step 2A)

Deposition of cells
(Step 2B&C)

Time: 10 - 45 min

Time: 24 - 48 h

Fluorescent labelling (Steps 3-9)

Time: 20 - 30min

Fiducial preparation
(Step 10)

Fiducialisation &
plunge freezing
(Steps 11 - 31)

Time: 5 - 10 min

Time: 20 min - 16h

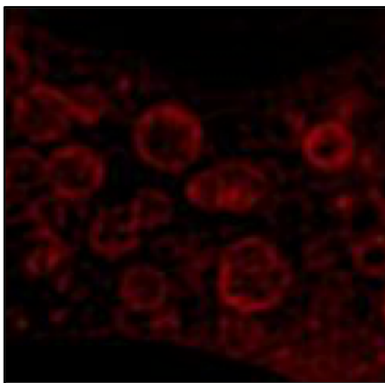
Cryo-sample evaluation (Steps 32 - 46)

Time: 10 - 30 min

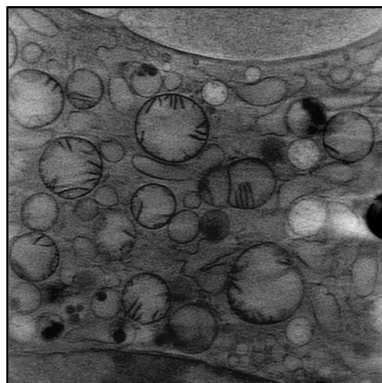
Cryo-sample mapping (Steps 47 - 54)

Time: 30 - 40 min

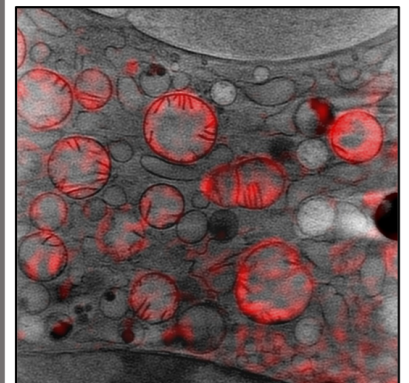
Super-
resolution
fluorescence
(cryoSIM)

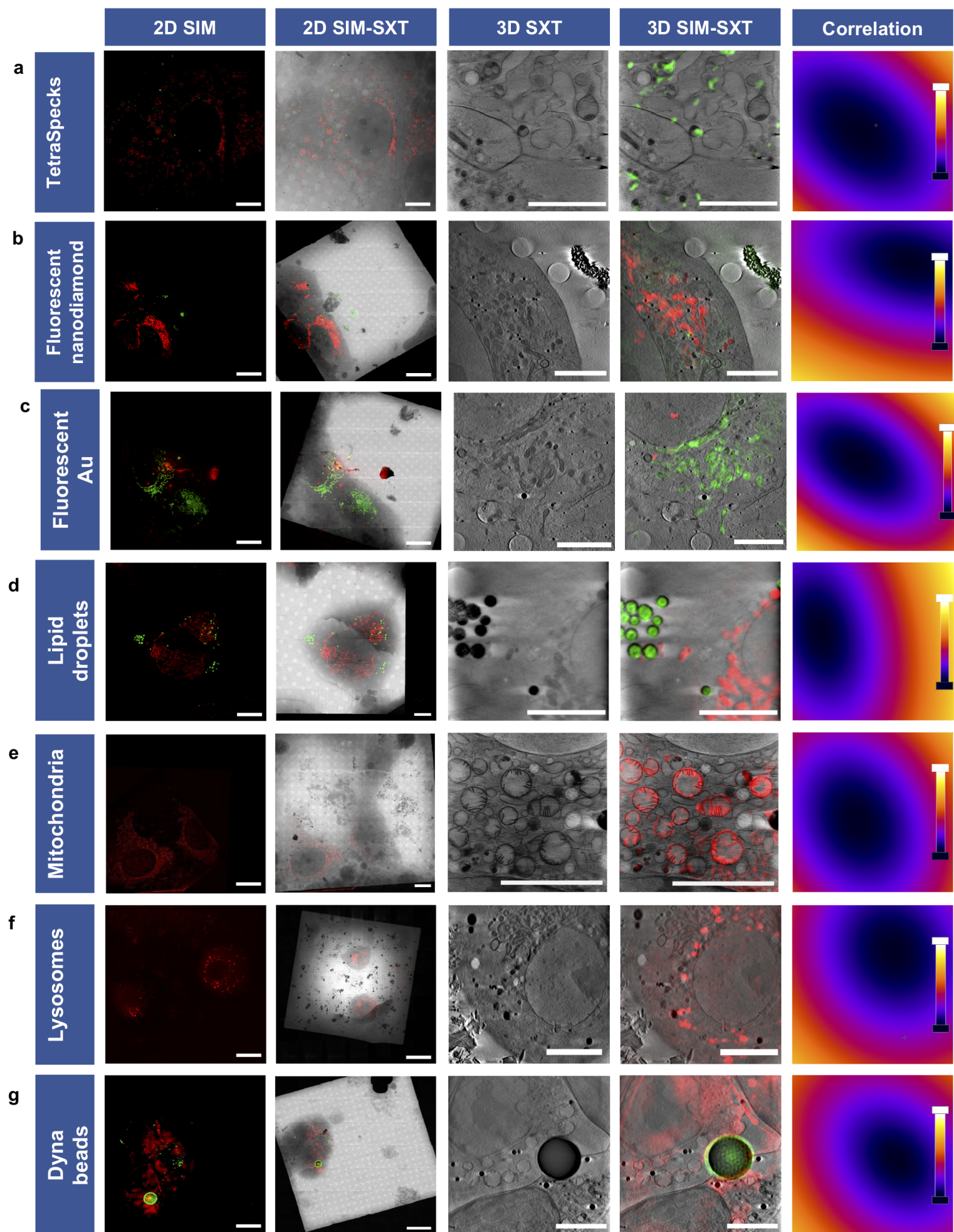


Soft X-ray
Tomography
(cryoSXT)

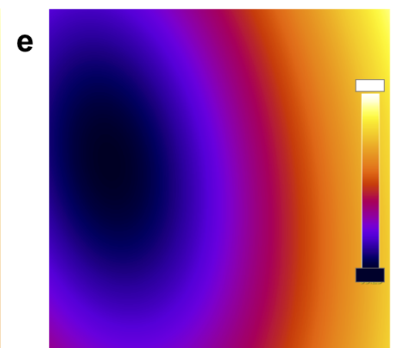
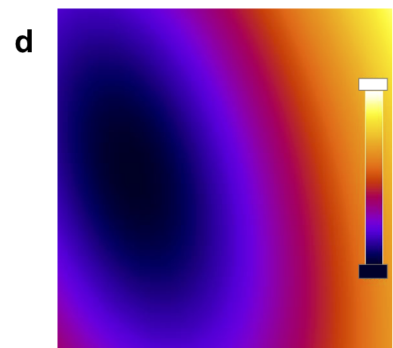
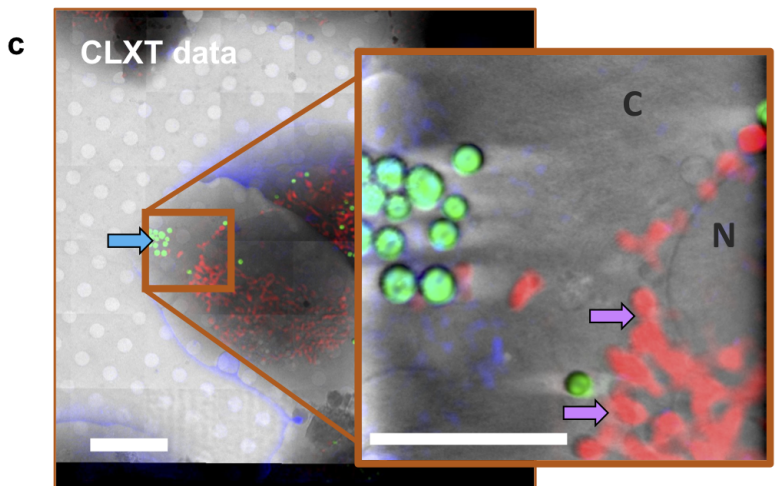
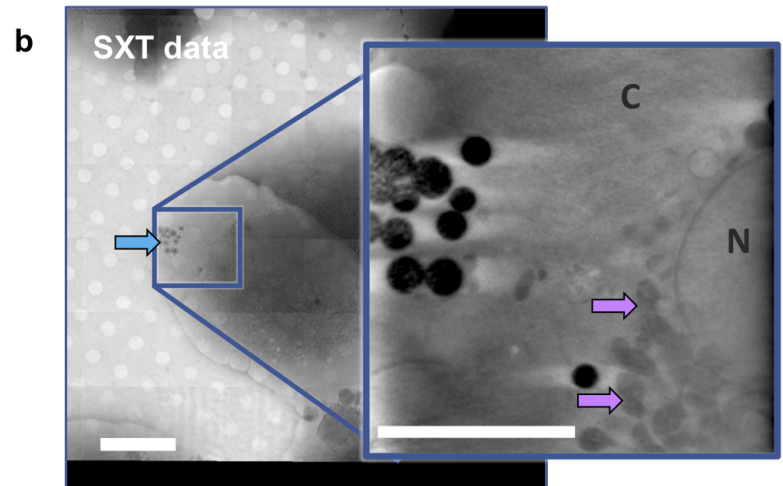
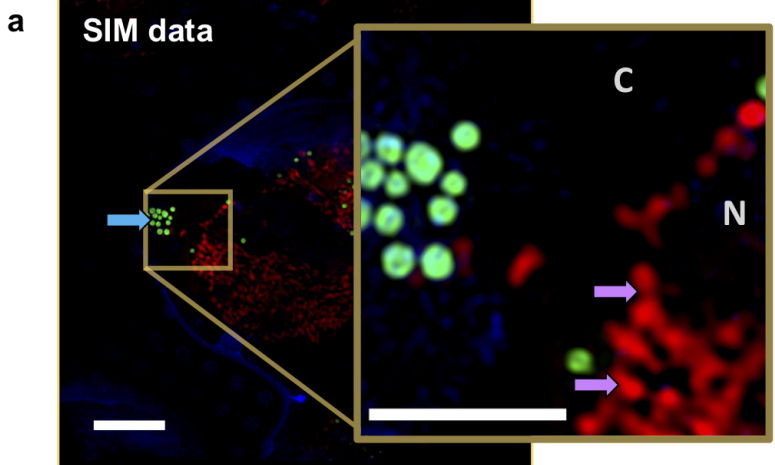


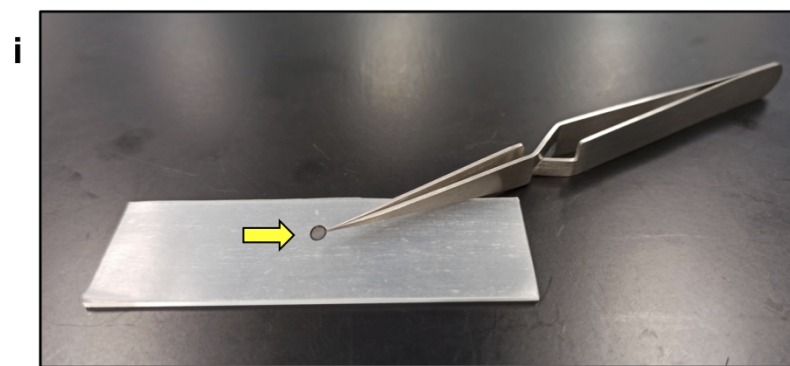
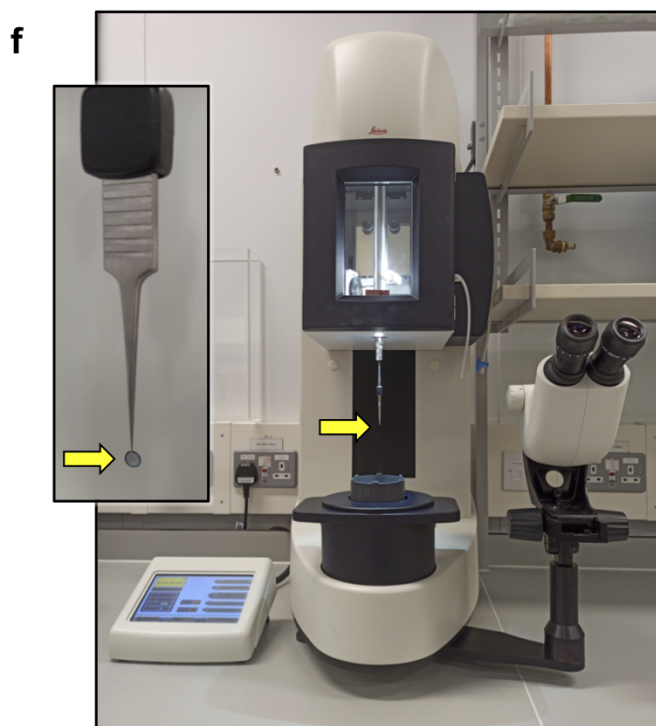
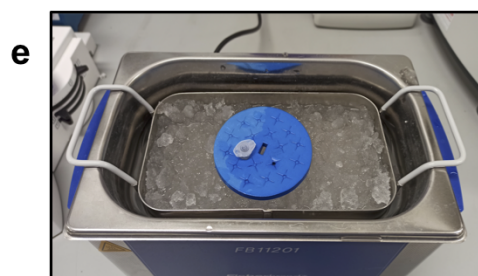
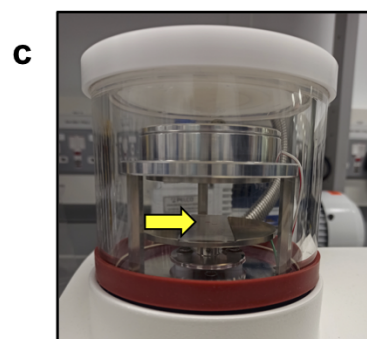
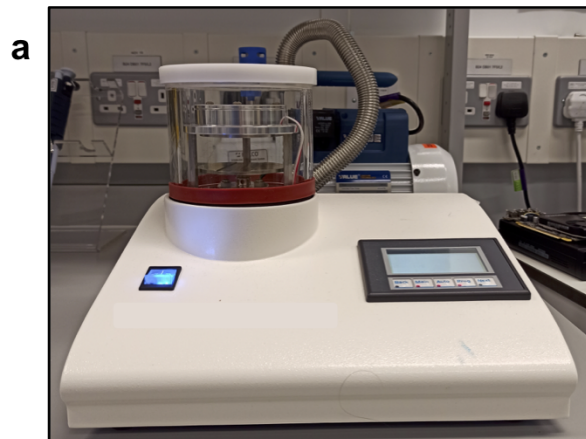
CLXT
Correlated
data





Criteria Fiducials	Market availability	Uniformity of distribution in sample	Fluorescence	Background auto-fluorescence	Stability during data collection	Batch variability	X-ray absorption	Automated X-ray processing potential	2D correlation (including brightfield)	Rough alignment 3D	Fine alignment 3D
Au Nanoparticles	✓	✓			✓		✓	✓	✓		
TetraSpecks	✓	✓	✓		✓	✓					✓
Fluorescent nanodiamonds					✓	✓	✓	✓	✓		✓
Fluorescent Ag nanoparticles			✓	✓		✓					
Fluorescent Au nanoparticles		✓	✓	✓	✓		✓	✓	✓	✓	✓
Lipid droplets.	✓		✓	✓	✓	✓	✓	✓	✓	✓	
Mitochondria	✓	✓	✓	✓	✓	✓	✓		✓	✓	
Nucleus	✓	✓	✓	✓	✓	✓	✓		✓		
Lysosomes	✓		✓	✓	✓	✓				✓	
Dynabeads	✓		✓	✓	✓	✓	✓		✓	✓	

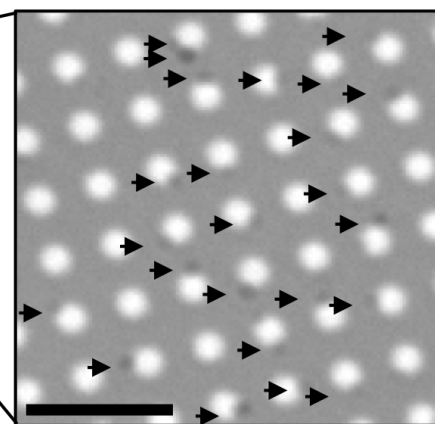
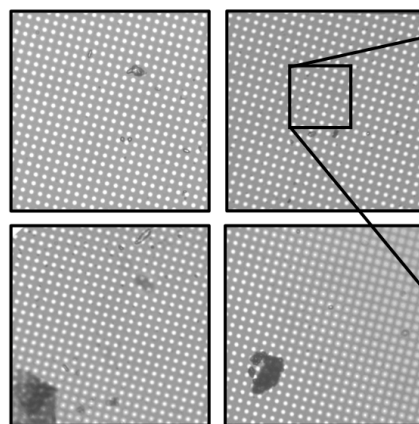
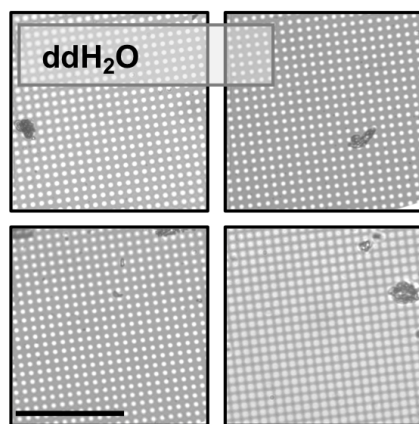




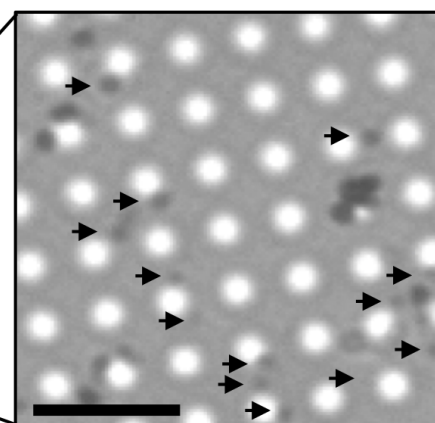
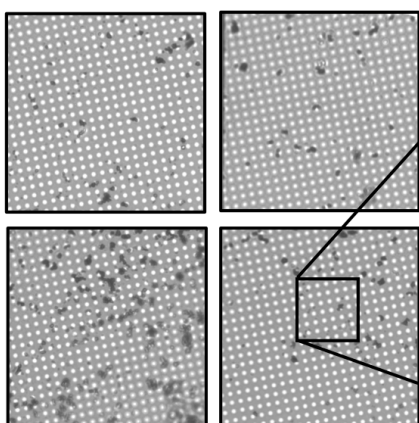
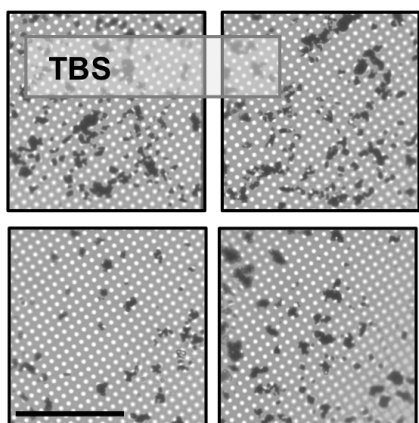
Before sonication

After sonication

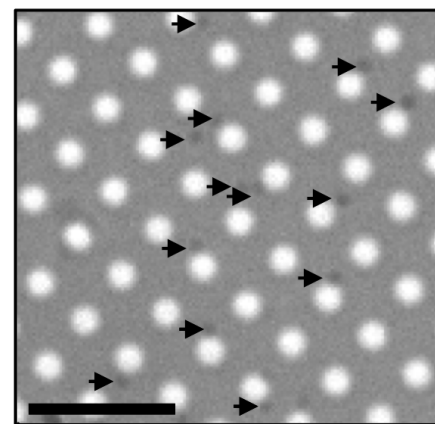
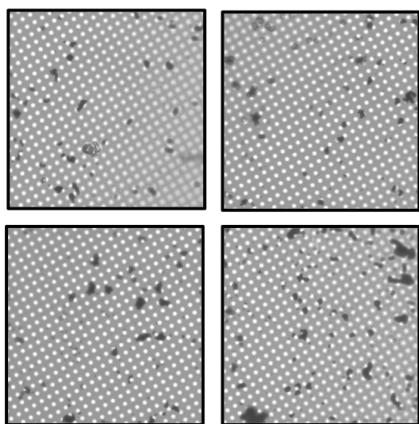
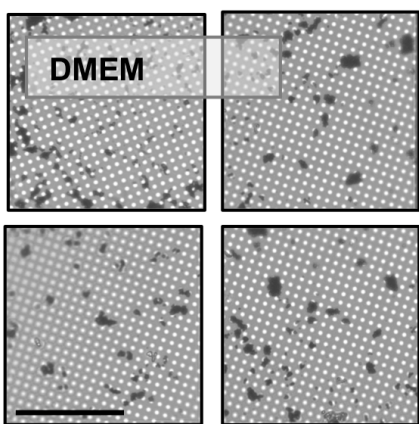
a



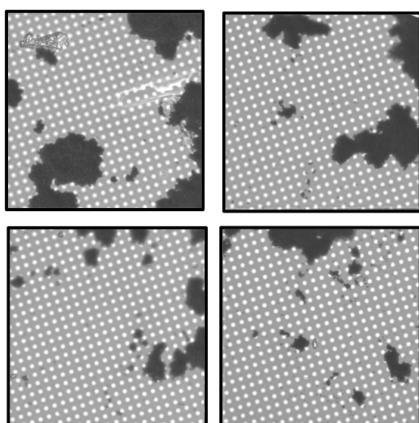
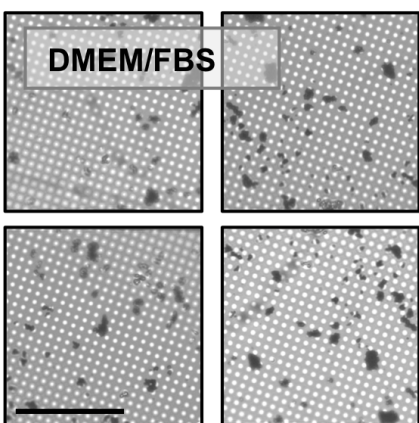
b



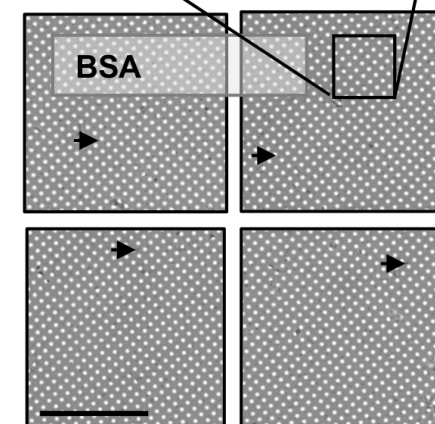
c

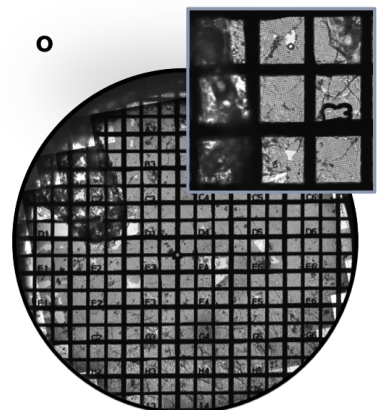
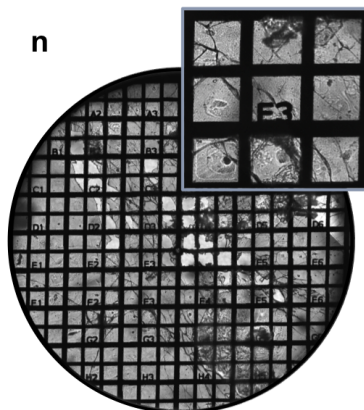
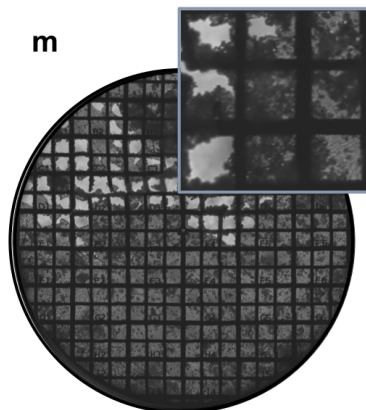
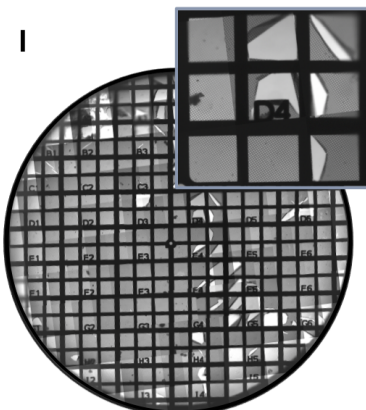
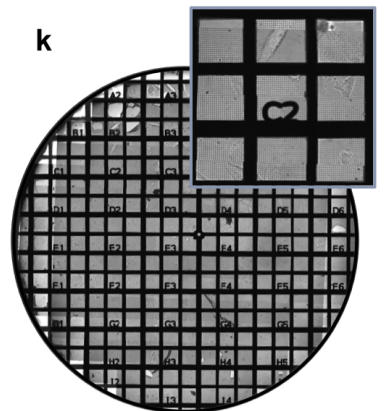
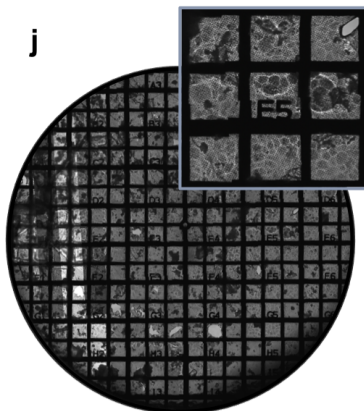
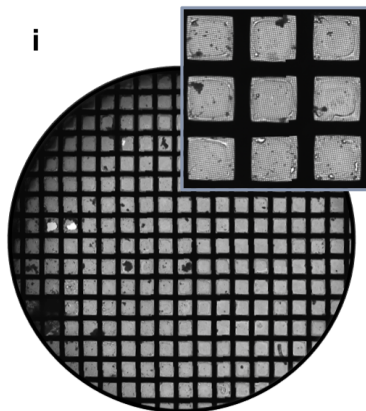
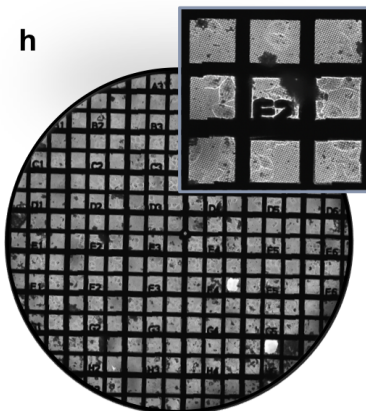
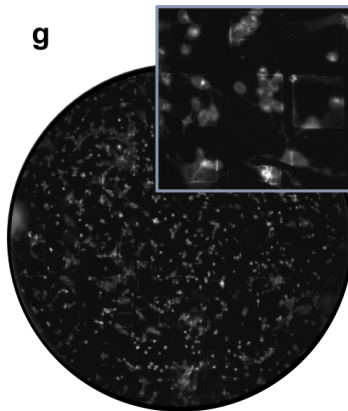
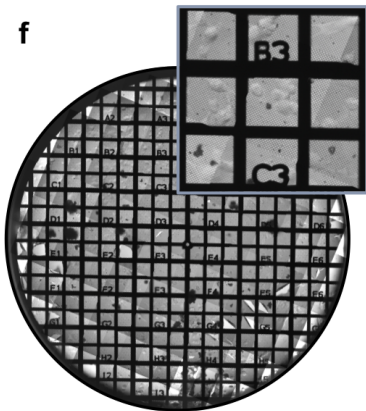
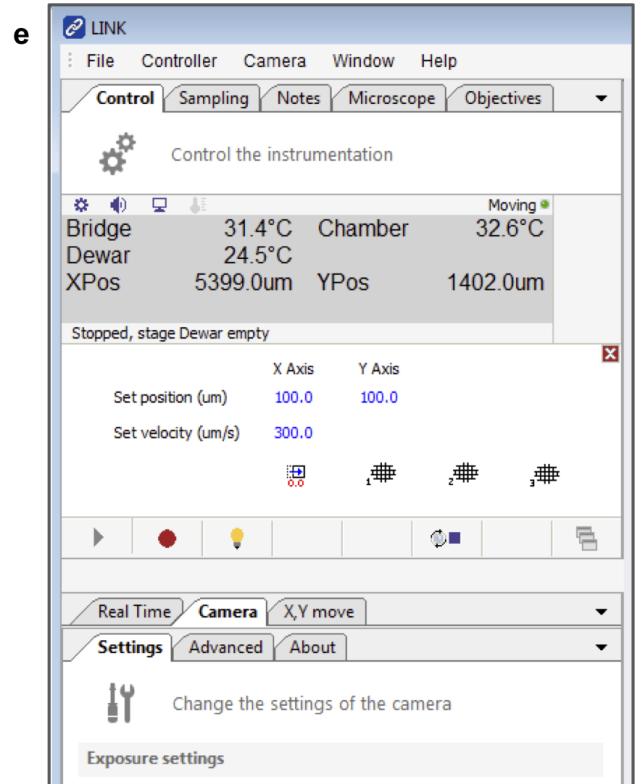
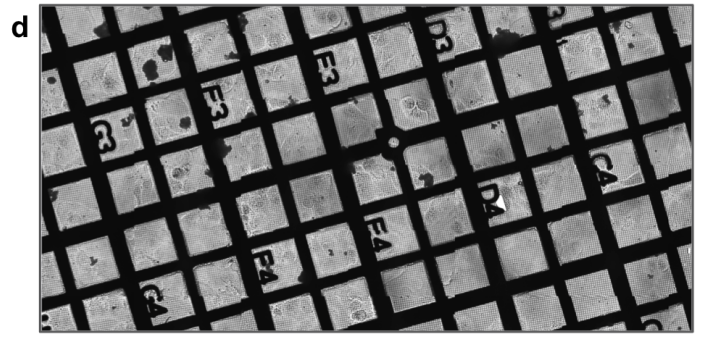
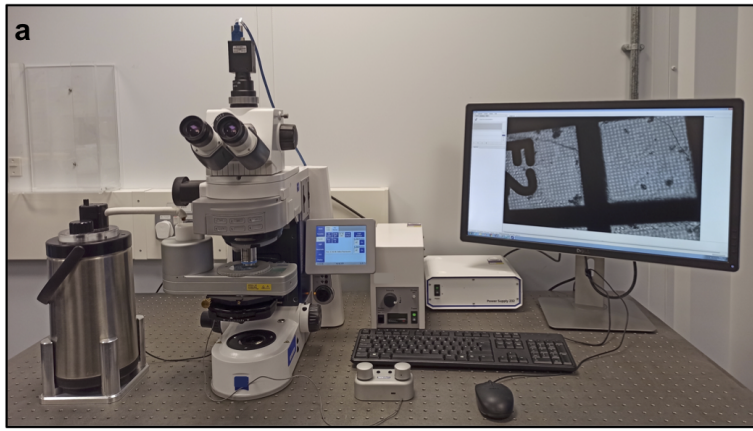


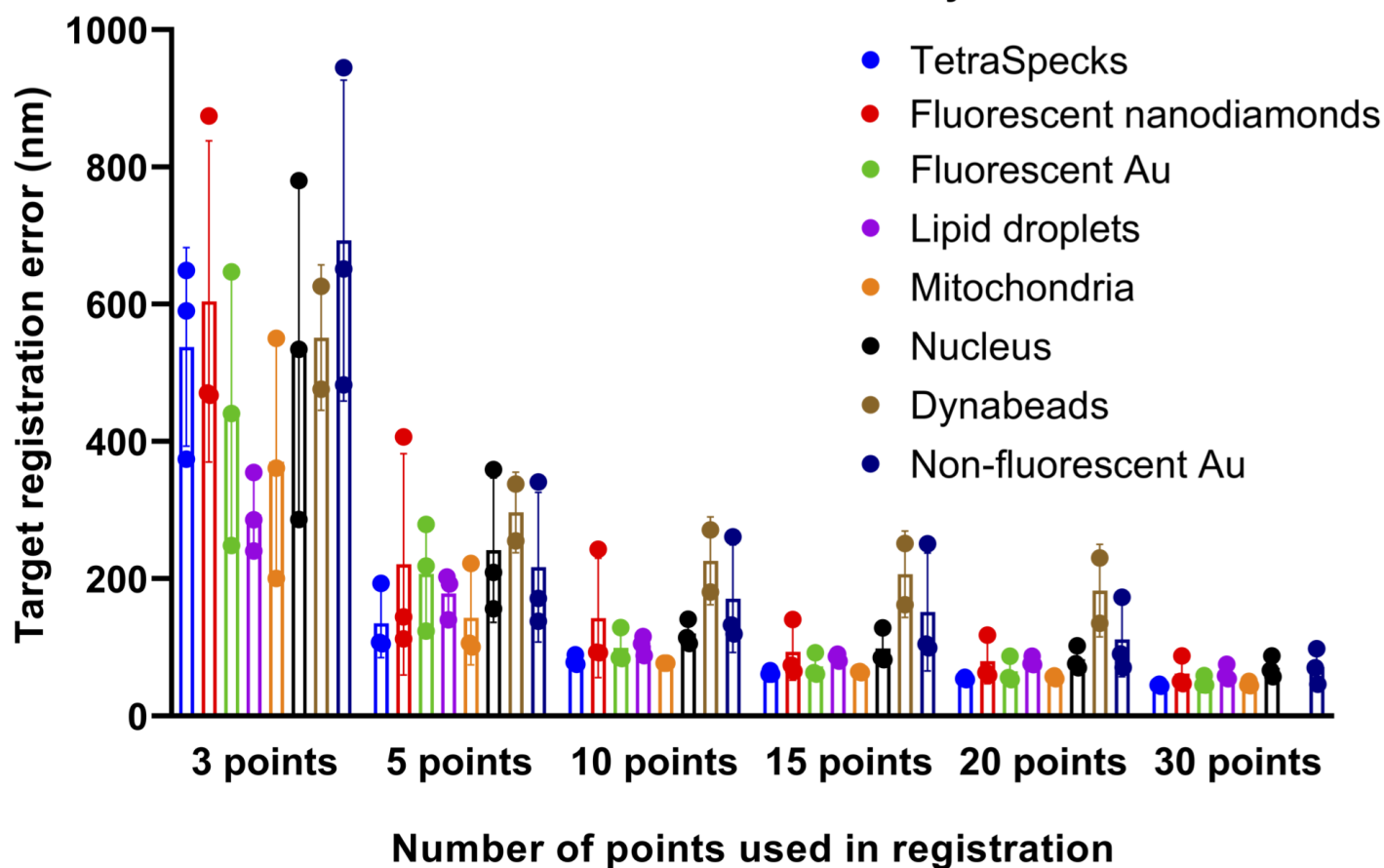
d



e





a**2D correlation accuracy****b****3D correlation accuracy**